Biol Cybern (2010) 102:155–176
DOI 10.1007/s00422-009-0360-3

ORIGINAL PAPER

Biological Cybernetics

A population level computational model of the basal ganglia that generates parkinsonian local field potential activity

George L. Tsirogiannis · George A. Tagaris · Damianos Sakas · Konstantina S. Nikita

Received: 3 June 2009 / Accepted: 14 December 2009 / Published online: 30 December 2009

Abstract Recordings from the basal ganglia's subthalamic nucleus are acquired via microelectrodes immediately prior to the application of Deep Brain Stimulation (DBS) treatment for Parkinson's Disease (PD) to assist in the selection of the final point for the implantation of the DBS electrode. The acquired recordings reveal a persistent characteristic beta band peak in the power spectral density function of the Local Field Potential (LFP) signals. This peak is considered to lie at the core of the causality–effect relationships of the parkinsonian pathophysiology. Based on LFPs acquired from human subjects during DBS for PD, we constructed a computational model of the basal ganglia on the population level that generates LFPs to identify the critical pathophysiological alterations that lead to the expression of the beta band peak. To this end, we used experimental data reporting that the strengths of the synaptic connections are modified under dopamine depletion. The hypothesis that the altered dopaminergic modulation may affect both the amplitude and the time course of the postsynaptic potentials is validated by the model. The results suggest a pivotal role of both of these parameters to the pathophysiology of PD.

G. L. Tsirogiannis (✉) · K. S. Nikita
Biomedical Simulations and Imaging Laboratory, School of Electrical and Computer Engineering, National Technical University of Athens, 9 Iroon Polytechneiou Street, 15773 Athens, Greece
e-mail: tsi@biosim.ntua.gr

G. A. Tagaris
Department of Neurology, "G. Gennimatas" General Hospital of Athens, 154 Mesogeion Avenue, 11527 Athens, Greece

D. Sakas
Parkinson's Disease Surgical Treatment Unit, Department of Neurosurgery, University of Athens, "Evangelismos" Hospital, 45–47 Ipsilantou Street, 10675 Athens, Greece

Keywords Basal ganglia · Beta band peak · Dopamine modulation · Local field potentials · Parkinson's disease · Population level models

1 Introduction

The basal ganglia are a subcortical group of nuclei involved in motor and mental tasks (Haber 2008; Smith and Wichmann 2008). The group comprises six nuclei: the striatum, which is considered to be functionally separated into the D1 and D2 segments (Bolam et al. 2000), the globus pallidus external segment (GPe), the globus pallidus internal segment (GPi), the subthalamic nucleus (STN), and the substantia nigra, which is separated in the pars compacta (SNc) and pars reticulate (SNr) segments (Smith et al. 1998; Pollack 2001). It is established that the basal ganglia play a pivotal role in movement disorders and psychiatric diseases (Utter and Basso 2008). That, together with the success of deep brain stimulation (DBS) treatment for Parkinson's disease (PD) (Limousin et al. 1995), has drawn particular focus to their pathophysiology. During typical operations of this kind, microelectrode recordings (MERs) are acquired from the subthalamic nucleus (STN) to assist in the selection of the final point for the fixation of the implanted electrode (Benazzouz et al. 2002; Priori et al. 2003). These recordings have revealed a characteristic persistent feature of PD, namely, a prominent peak in the beta band of frequencies of the power spectral density (PSD) function of the STN's local field potential (LFP) signals. This peak is considered to emerge as the projection of widespread synchronized beta band oscillations of the underlying neuronal elements (Boraud et al. 2005; Brown and Williams 2005; Weinberger et al. 2006). The peak is currently thought to be a significant expression of the pathophysiology of the basal ganglia in PD,

associated with the impairment of movement (Brown 2003; Dostrovsky and Bergman 2004; Chen et al. 2006).

The exact pathophysiological causes for the appearance of the beta synchronized oscillations remain obscure. Experimental studies have assigned their root cause to chronic dopamine depletion (Sharott et al. 2005; Mallet et al. 2008). Weinberger et al. (2006) have unveiled a relation between the degree of beta oscillatory activity and the magnitude of the response of the basal ganglia to dopaminergic agents. Moreover, some studies have shown a reduction in the height of the peak by dopaminergic therapy or DBS (Kuhn et al. 2006; Wingeier et al. 2006). In a computational modeling study, Terman et al. (2002) have simulated a small network of the GPe and STN to explain the emergence of oscillatory activity. Oscillations were found in the output of these nuclei when the striatal input to the GPe was increased and the intra-GPe inhibition was weakened. More detailed considerations have been presented in Bevan et al. (2002). There, the importance of special neuronal properties of the STN and the GPe for the prevalence of oscillatory activity has been stressed. Particular focus has been given to the after-hyperpolarization rebound burst response noted in STN. Bevan et al. have also discussed two alternative explanations for the source of the synchronized oscillatory activity. That is supposed to be either generated within the STN–GPe network, or imposed on the basal ganglia by external sources, such as the cortex.

This study aims to shed light on the critical pathophysiological alterations that lead to the emergence of the characteristic parkinsonian beta band peak in the PSD function of the STN's LFPs. To this end, we constructed and used a computational model of the basal ganglia, which generates artificial LFPs from the STN and reproduces a putative parkinsonian condition by proper modification of its parametric configuration.

The modeling formalism of the proposed computational model of the basal ganglia follows the population level paradigm. That has originally been described by Lopes da Silva et al. (1974, 1976) for the study of the mechanisms that generate alpha rhythm in the cortex. Population level models of this kind are based on the idea that the functioning of a large number of similar neighboring neurons belonging to the same nucleus or region can be summarized by the characteristics of one single homogenized structure. That is why these models are also called lumped parameter models. Apart from the studies of Lopes da Silva et al., Freeman has also used them for the study of the olfactory system's reaction to external cues (Freeman 1978). Other similar population level-based approaches include the studies of Jansen et al., who have utilized a population level model of the cortex to produce visual evoked potentials by a single cortical column (Jansen et al. 1993) or by two coupled columns (Jansen and Rit 1995). Also, Wendling et al. (2000) have established the relevance of lumped-parameter models in the analysis of depth-EEG signals from epileptic patients. Further, they have presented such a model (Wendling et al. 2002) to explain the generation of epileptic activity by impaired GABAergic dendritic inhibition. Finally, an approach that represents LFPs generated by coupled neuronal populations distributed over a patch of the neocortex has been published (Cosandier-Rimele et al. 2007).

In our approach, first, we defined the architecture of a population level model of the basal ganglia. The outputs of the model are the LFP signal of the STN and the mean firing rates of all the nuclei. Next, we selected putatively normal values for its parameters, according to reports on them in the literature. After evaluating the model's outputs with the baseline configuration, which is thought to correspond to a normal rest state condition, we properly altered the configuration to reproduce the parkinsonian condition.

The latter was defined by the expected increase in the firing rates of the D2 segment of the striatum, the GPi, and the STN, relative to the mean normal levels. In contrast, the D1 segment of the striatum and the GPe are expected to fire less in PD (Bergman and Deuschl 2002; Wichmann and DeLong 2006). Moreover, as already described, LFP recordings from the STN have revealed the expression of a significant prominent beta band peak in their PSD function. The combination of the presence of the beta band peak and the plausibility of the firing rate modifications define the targeted parkinsonian behavior of the model.

The types of alterations that were assumed to form the modified parkinsonian parametric configuration of the model were extracted by experimental studies that have revealed the role of the lack of dopamine in the modulation of the strength of the PSPs. The cortical projection to the striatum is thought to be modified in PD, toward weakened and enhanced influences to the D1 and the D2 segments, respectively (West and Grace 2002). In the STN, both inhibitory and excitatory projections seem to be enhanced under dopamine-depleted states (Shen and Johnson 2000; Shen et al. 2003; Floran et al. 2004). Finally, in the GPe, it has been found that the inhibitory connection from the striatum is enhanced in such states (Cooper and Stanford 2001), and the input from the STN is hyperactive (Johnson and Napier 1997). Since the parkinsonian condition comes up as a consequence of the lack of dopamine, we modified the synaptic parameters of the model, reflecting that altered modulation of the PSP strength, to simulate the pathophysiological state.

Although the synaptic strength modulation by dopamine depletion is mainly attributed to the amplitudes of the PSPs, we assumed that the time course of the PSPs might also be altered. The idea of the significance of the PSP time courses in neural system functionality has been examined in other modeling studies as well. Rinzel et al. (1998) have studied the influence of PSP time courses on the activity patterns

of neuronal networks. Choe and Miikkulainen (2003) have modeled the synchronizing effects of the PSP time courses. Also, experimental data have disclosed the synchronizing properties of the synaptic time course on networks of bursting neurons (Elson et al. 2002). Through the proposed model, we validated the hypothesis that the time courses of the PSPs in the basal ganglia may be significant for the pathophysiological synchronization expressed by the presence of the beta band peak in PD.

In the following, we first describe the type of the actual recorded signals from parkinsonian subjects that have been used to assess the value of the proposed model. Then, the population level modeling paradigm followed by the model is outlined, and the selection of the baseline values of the parameters is explained. Before presenting and discussing the results, the methodology of altering the configuration of the model toward the parkinsonian state is addressed.

2 Material

In order to design and evaluate the simulations of the proposed model, we used LFP signals derived from MERs recorded from the STN of four human subjects during typical DBS intervention for PD. The recordings are routinely performed to aid the selection of the final electrode fixation point (Benazzouz et al. 2002). The acquisition took place prior to the final implantation of the stimulating electrode and after overnight withdrawal of anti-parkinsonian drugs. The recording session consisted of moving a microelectrode along a predefined line grid of points that included the theoretical target. The latter was the Posterior part of the STN and was approximately defined on the patients' Magnetic Resonance Imaging (MRI) data prior to the DBS procedure.

The signals were acquired by means of an array of five microelectrodes in cross formation, known as Ben Gun (Benabid et al. 1991), entering in parallel into the brain tissue. The different electrodes are referenced by an anatomical term indicating position, namely, Central, Anterior, Posterior, Lateral, and Medial. The distance between the tips of the peripheral electrodes and the central one is 2 mm. Each MER was acquired for a 10-s period using a sampling frequency of 24 KHz. MERs obtained in this way are information rich, containing both LFPs and spiking activity. These types of activity are considered to be contained in the low and high range of the frequency spectrum, respectively (Trottenberg et al. 2007). That is due to the low-pass filtering properties of the brain tissue (Bedard et al. 2006), which allow low frequencies to travel relatively far from the source via volume conduction. In contrast, high frequencies attenuate rapidly with distance. Logothetis et al. (2007) have suggested an alternative explanation for the ability of the low frequencies to travel further, namely, that the high amplitude of the low frequencies allows them to attenuate less with distance. However, their suggestion points to the same result. Thus, low frequencies arise from wider neighboring regions, whereas high frequencies stem from only a few neurons around the electrode's tip (Nunez and Srinivasan 2006). All these together explain why LFPs mainly reflect regional synaptic activity and are extracted from MERs as their low frequency content (Liu 2003). Usually, the cut-off frequency used for separating these two kinds of activity via low-pass filtering is around 100 Hz (Brown et al. 2002; Walters et al. 2006; Chen et al. 2006). Similarly, the LFP signals used in this study are obtained from the recorded MERs by applying a low-pass filter with 100 Hz cut-off frequency, followed by a down-sampling at 1 KHz.

The line grid of points in the brain where MERs are acquired varies for each patient, but there is a general pattern that dictates a range between −4 and +2 mm, with 0.5 mm steps (the reference 0 mm is the pre-determined target inside the STN as defined on MRI scans). The probability of a recording to originate from the STN gets higher when it corresponds to points closer to the 0 mm point. Thus, since in this study we are interested in recordings from the STN that exhibit a beta peak in their PSD function, we only considered recordings from the Central electrode in the range from −2 to +2 mm points. After evaluating their PSD function (using the Welch's modified periodogram method) and extracting the ratio of the total energy content of the beta peak versus the total energy content in the range 0–100 Hz, we selected representative LFP signals that expressed a beta peak for positions of the Central electrode between −1 and 1 mm. The representative signals exhibited the higher ratios.

All the available recordings were acquired from four subjects with PD (S1–S4), who had undergone unilateral electrode implantation for DBS. The gender, age, disease time, and off drugs UPDRS score details of the subjects are presented in Table 1. All the subjects were predominantly akinetic and were kept awake and without medication during surgery. Table's 1 last column also reports the specific point in frequency that the beta peak is found for each subject. The PSD functions of the representative S1–S4 LFP recordings are depicted in Fig. 1.

Despite the fact that the beta band is mainly considered to lie in the 12–30 Hz range, our recordings revealed that two of the subjects expressed the beta band at frequencies above 30 Hz (S1: 32 Hz, S4: 38 Hz). In the following, we will retain the 12–30 Hz consideration for the beta band, but we will also show how the model can express peaks at frequencies outside that range, in the alpha (8–12 Hz) and gamma (>30 Hz) bands.

Table 1 Age and disease details of the four subjects with PD (S1–S4), from whom the STN's LFP recordings were acquired during the DBS electrode implantation procedure

Subject identifier	Gender	Year of birth	Disease start year	UPDRS (off drugs)	Beta band peak frequency (Hz)
S1	Male	1946	1993	38	32
S2	Male	1935	1987	54	24
S3	Male	1957	1994	32	28
S4	Male	1940	1994	37	38

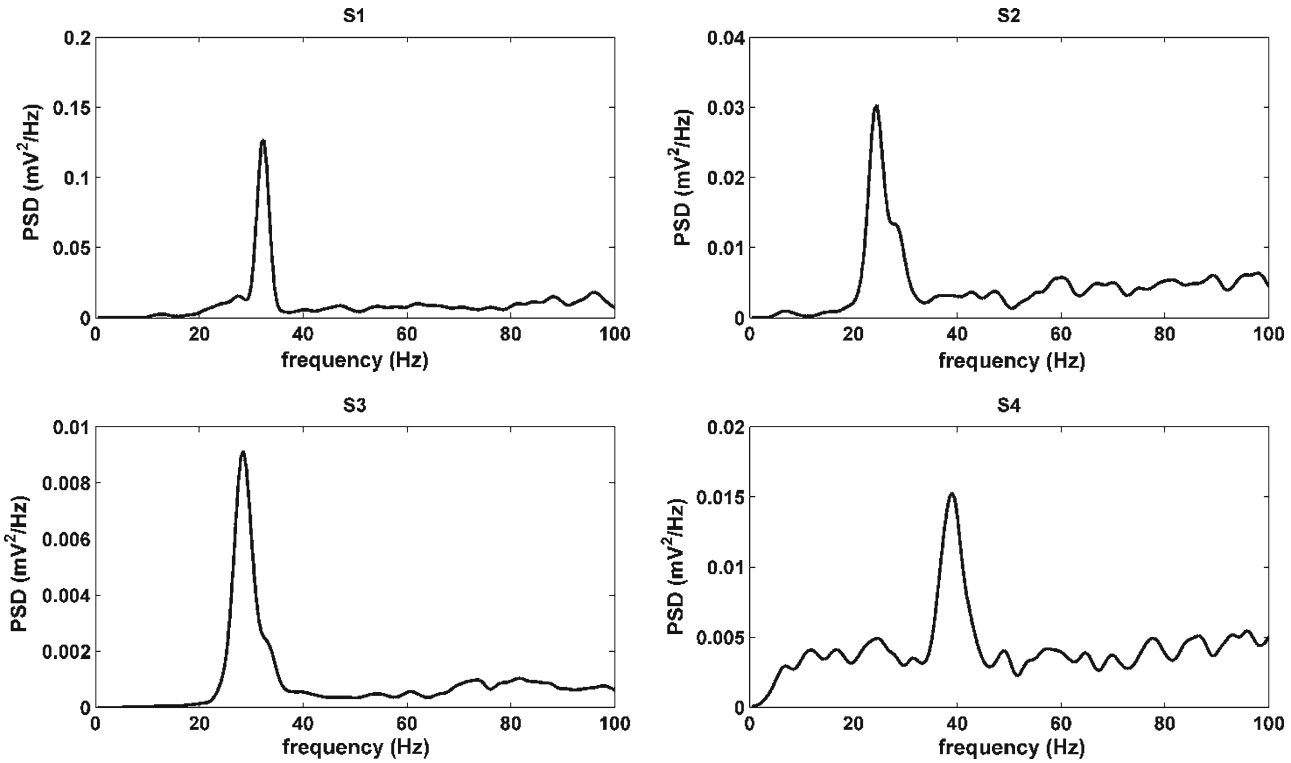

Fig. 1 Representative PSD functions of the LFP signals from the four subjects (S1–S4), with a prominent peak in the beta band. The peaks are expressed in different points in the beta band of frequencies. In general, for all of each subject's LFP signals that express a spectral beta band peak, that prominent peak appears at the same point in frequencies (see Sect. 4)

3 Methods

3.1 Population level architecture

The mathematical basis of the population level formulation used in this study has originally been described by Lopes da Silva et al. (1974, 1976). In those studies, as well as in the more recent ones that adopted the population level formulation (Jansen et al. 1993; Jansen and Rit 1995; Wendling et al. 2002), the models included no transmission delays. Recently, several studies have addressed the role of the delays in the synchronization of brain activity (Vibert et al. 1994; Gopalsamy and Leung 1996; Vibert et al. 1998; Freeman 2000). That is why, in this study, the original population level formulation was slightly altered, to also incorporate transmission delays in the synaptic connections.

The general architectural block diagram of the formulation is schematically depicted in Fig. 2, for an exemplary population that receives one excitatory and one inhibitory input. Each input (x^+ is the excitatory and x^- the inhibitory one) represents the mean firing rate of the corresponding presynaptic population and is measured in spikes/s. Before reaching the postsynaptic population, the inputs are multiplied by scalar values, C^+ and C^-, respectively, representing the number of physical synaptic contacts between two connected populations. The resulting x^+C^+ and x^-C^- products reflect the excitatory and inhibitory influences, respectively, of the corresponding presynaptic populations. These influences

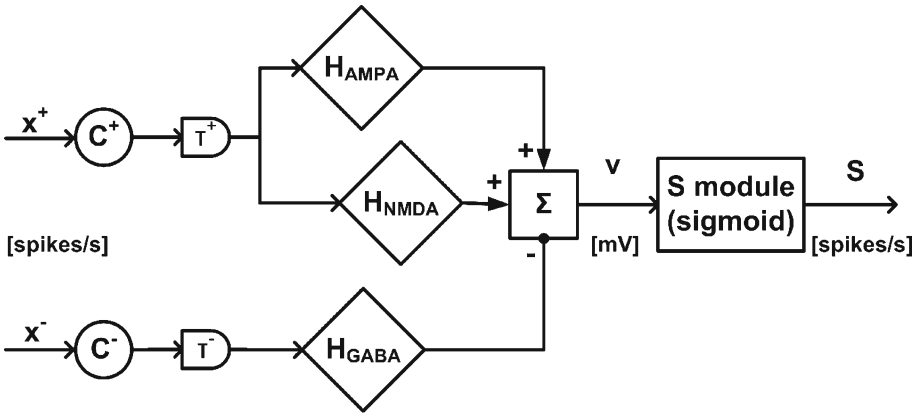

Fig. 2 Example of a general population according to the population level paradigm. Input firing rates (x^+, x^-), measured in spikes/s, come from presynaptic populations and are weighted by the corresponding C parameters (pictured as *circles*: C^+, C^-), representing the mean number of physical synaptic contacts. The input activities reach the H modules (diamonds) after the respective transmission delays (τ^+, τ^-). The H modules generate PSPs, measured in mV, from the input activities, according to AMPA, NMDA, and GABA receptor properties. The total PSP of the population is derived as the sum of the outputs of the H modules and drives the S module (*rectangle*). The latter applies a sigmoid function to calculate the output firing rate of the population, measured in spikes/s

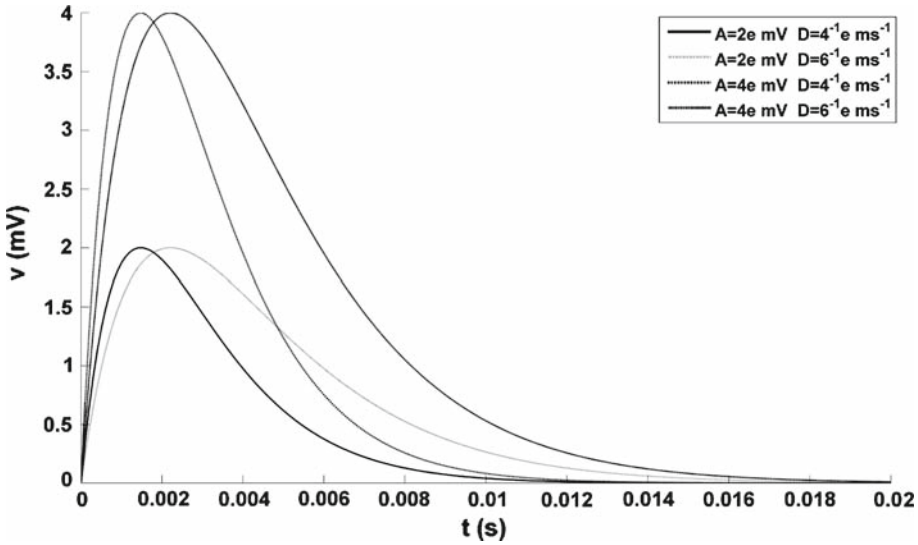

Fig. 3 The alpha PSP form derived by (2), to which the responses of the H module are equivalent. The A and D parameters of (1) are, respectively, proportional and inversely proportional to the amplitude and the time constant of the PSP, (e denotes the exponential constant)

reach the postsynaptic population after the respective τ^+ and τ^- time delays, imposed by the time needed for the transmission of the activities via the neuronal axons, from the source population to the target (axonal delays). There, they are transformed to mean postsynaptic potentials by the H modules, which concentrate all the actual presynaptic and postsynaptic modulations of the synaptic activities. For the purposes of this study, we considered only glutamatergic excitatory connections, mediated by AMPA and NMDA receptors and GABAergic inhibitory connections, mediated by $GABA_A$ receptors (Gotz et al. 1997; Ravenscroft and Brotchie 2000).

Therefore, the H modules can be of three types, according to which type of receptor mediates the generation of the postsynaptic potential: H_{AMPA}, H_{NMDA} and H_{GABA}. The general equation used for the H transformation, regardless of the particular receptor type, is the following second-order differential equation:

$$\ddot{H}(t) = ADCx(t-\tau) - 2D\dot{H}(t) - D^2H(t) \quad (1)$$

In (1), x, C, and τ represent the presynaptic populations' mean firing rate, the synaptic contact parameter, and the axonal delay, respectively.

The form of the PSP generated by (1) is equivalent to the alpha function originally proposed by Van Rotterdam et al. (1982):

$$v(t) = ADte^{-Dt} \quad (2)$$

In (2), $v(t)$ is the PSP elicited by a single presynaptic spike at time $t = 0$. As Fig. 3 depicts, the amplitude (maximum height) of the PSP is equal to $A \cdot e$, and the time constant is

equal to e/D, where e is the exponential constant. Thus, A is proportional to the amplitude, and D is inversely proportional to the time constant of the PSP. The A and D parameters are characteristics of the receptor function and may take distinct values for AMPA, NMDA, and GABA receptors. Based on (1), the H_{AMPA}, H_{NMDA}, and H_{GABA} modules are described by the following equations:

$$\begin{aligned}\ddot{H}_{\mathrm{AMPA}}(t) &= A_{\mathrm{AMPA}} D_{\mathrm{AMPA}} C^{+} x^{+}(t-\tau^{+}) \\ &\quad -2D_{\mathrm{AMPA}} \dot{H}_{\mathrm{AMPA}}(t) \\ &\quad -{D_{\mathrm{AMPA}}}^{2} H_{\mathrm{AMPA}}(t) \end{aligned} \tag{3a}$$

$$\begin{aligned}\ddot{H}_{\mathrm{NMDA}}(t) &= A_{\mathrm{NMDA}} D_{\mathrm{NMDA}} C^{+} x^{+}(t-\tau^{+}) \\ &\quad -2D_{\mathrm{NMDA}} \dot{H}_{\mathrm{NMDA}}(t) \\ &\quad -{D_{\mathrm{NMDA}}}^{2} H_{\mathrm{NMDA}}(t) \end{aligned} \tag{3b}$$

$$\begin{aligned}\ddot{H}_{\mathrm{GABA}}(t) &= A_{\mathrm{GABA}} D_{\mathrm{GABA}} C^{-} x^{-}(t-\tau^{-}) \\ &\quad -2D_{\mathrm{GABA}} \dot{H}_{\mathrm{GABA}}(t) \\ &\quad -{D_{\mathrm{GABA}}}^{2} H_{\mathrm{GABA}}(t) \end{aligned} \tag{3c}$$

Equation 1 can be rewritten for simplicity as two first-order differential equations, using the intermediate variable $z(t)$:

$$\begin{cases} \dot{H}(t) = z(t) \\ \dot{z}(t) = ADCx(t-\tau) - 2Dz(t) - D^{2}H(t) \end{cases} \tag{4}$$

Accordingly, the Eqs. 3a–c can be rewritten in the form of (4), which will result in the description of the model as a set of first-order differential equations that can be solved by standard numerical algorithms.

In order to obtain the total PSP elicited to each population, the outputs of the H modules are summed. The summation preserves a + sign for the excitatory connections and a – sign for the inhibitory ones. With regard to the general population of Fig. 2, it is

$$v = H_{\mathrm{AMPA}} + H_{\mathrm{NMDA}} - H_{\mathrm{GABA}} \tag{5}$$

The total PSP v is measured in mV and is thought to represent the LFP signal that would be recorded from the population. That is because the LFPs are considered as the result of the summated synaptic activity of a relatively large number of neighboring neurons (Bullock 1997; Liu 2003). The biological plausibility of that is justified by the anatomical arrangement of the cells within the STN, which usually have their dendritic fields parallel to the long axis of the nucleus (Hamani et al. 2004; Brown and Williams 2005). Because of this open-field canonical organization, the generation of the extracellular field is summated over the whole of the population and not mutually canceled, as it would be in a random orientation (Johnston and Wu 1995). Therefore, the STN is considered to be a proper target for acquisition and model-based generation of LFPs.

As a final processing stage within a population, the utilized architecture assumes that the total PSP drives the mean output firing rate of the population (measured in spikes/s), via a sigmoid transformation. In Fig. 2, an S module is embedded to represent that transformation. The corresponding equation is

$$S(v) = \frac{S_{\max}}{1 + \exp(k(v_h - v))} \tag{6}$$

where $S_{\max}$ is the asymptotic maximum firing rate that can be achieved by the population, k is the sensitivity of the population to changes in the received PSP, and v_h is the PSP value needed for reaching the half of the maximum firing rate.

3.2 Basal ganglia model design and normal parametric configuration

In this study, the above described population level architecture has been adapted to model basal ganglia. Four out of the six nuclei of the basal ganglia have been explicitly included in the developed population level model, namely, the striatum, the GPe, the GPi and the STN. Each nucleus in the model was regarded as one single population, with the exception of striatum, for which each segment constitutes a population. The GPi is the output nucleus of the basal ganglia and does not project to the other nuclei, but it has been included to provide evidence for the functional state of the model, through the assessment of its mean firing rate output. The SNr, the other output structure of the basal ganglia, has been omitted since it is considered homologous to the GPi (Parent 1986). The SNc is thought to affect the physiology of the whole system through the dopamine produced by it (Smith and Kieval 2000). Thus, its effect is regarded to be modulatory, and it has been omitted by the explicit architectural structure of the model, playing a rather shadowed role.

The properties of each population were lumped into the sigmoid transformation of the S module (Fig. 2), as described above. The selection of the values of the parameters for the sigmoid functions of the form (6) was based on experimental studies that reported the active membrane properties of the main type of neurons constituting each nucleus. The information of interest is conveyed by standard firing frequency–input current (f–I) and input current–membrane voltage (I–V) curves. Such curves illustrate the maximum firing rate that can be achieved by a neuron type [the $S_{\max}$ parameter of (6)], as well as the membrane potential needed to drive the neuron to the half of the maximum firing rate [the v_h parameter of (6)]. The k parameter of (6) is an approximation of the slope of an assumed firing frequency – membrane potential (f–V) curve and can be calculated by the combination of the f–I and I–V curves.

In particular, both striatal segments express the same properties (Cepeda et al. 2008), and their values are calculated by the f–I and I–V curves as reported in Kita et al. (1985): $S_{\max}^{\mathrm{striatum}} = 300\,\mathrm{spikes/s}$, $k^{\mathrm{striatum}} = 0.3\,\mathrm{mV}^{-1}$, and $v_{\mathrm{h}}^{\mathrm{striatum}} = 27\,\mathrm{mV}$. The spontaneous firing rate of the striatal

neurons is reported to be close to zero, explaining the usual quiescence of those neurons under the normal rest states, in which the cortical input is not strong enough to make them sustain the firing. The total PSP needed to drive the population to firing rates greater than zero is around 8 mV (Kita et al. 1985), and this fact is satisfied by the particular selection of the parameters. For the STN, we used the published data of Nakanishi et al. (1987), which have been previously used by Gillies and Willshaw (2004) to constrain a similar sigmoid function as per (6), which reproduces the firing properties of the STN neurons. The authors of the latter provide the ranges for the k and v_h parameters in 0.1–0.3 mV^{-1} and 15–22 mV, respectively. In their study, they finally performed the simulations with $k = 0.3\,\mathrm{mV}^{-1}$ and $v_\mathrm{h} = 15\,\mathrm{mV}$. Here, we selected the middle values, i.e., $k^\mathrm{STN} = 0.2\,\mathrm{mV}^{-1}$ and $v_\mathrm{h}^\mathrm{STN} = 18.5\,\mathrm{mV}$. The maximum firing frequency $S_\mathrm{max}^\mathrm{STN}$ is thought to be 500 spikes/s, and this value is retained in this study. In Gillies and Willshaw (2004), the GPe's firing properties have also been lumped into a sigmoid function with $S_\mathrm{max} = 100$ spikes/s, $k = 0.2\,\mathrm{mV}^{-1}$, and $v_\mathrm{h} = 10\,\mathrm{mV}$, as retrieved from studies in guinea pigs (Nambu and Llinas 1994). The authors of Gillies and Willshaw (2004) have probably considered the type I neurons of GPe, according to the categorization of Nambu and Llinas (1994). However, the corresponding type I neurons in the Cooper and Stanford (2000) study of the rat's globus pallidus are reported to exhibit higher firing rate responses, at 350 spikes/s at maximum. In addition, type II neurons in the GPe are almost half as many as the type I neurons, meaning that they may also play a significant role in GPe's responses. Type II neurons are reported to be able to reach 200 spikes/s firing in guinea pigs (Nambu and Llinas 1994) and 440 spikes/s in rats (Cooper and Stanford 2000). The previously mentioned published data that have been selected to constrain the parameters of the sigmoid functions of the striatal D1, D2, and STN populations came from studies in rats. That is why we finally selected to use the data published in Cooper and Stanford (2000), which also originated from rat subjects, to constrain the $S_\mathrm{max}^\mathrm{GPe}$ parameter. Thus, we finally selected $S_\mathrm{max}^\mathrm{GPe} = 400$ spikes/s, $k^\mathrm{GPe} = 0.2\,\mathrm{mV}^{-1}$ and $v_\mathrm{h}^\mathrm{GPe} = 10\,\mathrm{mV}$. The GPi's maximum firing rate $S_\mathrm{max}^\mathrm{GPi}$ was constrained by the report of Nakanishi et al. (1990) on the electrical membrane properties of the rat entopeduncular nucleus neurons [structure that is homologous to the GPi of the primates (Parent and Hazrati 1995)] in which study the type I neurons identified were the most prominent in numbers and could exhibit a maximum firing rate of 300 Hz. Owing to the lack of data in the literature about the k^GPi and $v_\mathrm{h}^\mathrm{GPi}$ parameters, we used the same values as for GPe, based on the homologous cytoarchitecture of the two structures (Carpenter et al. 1981). As described in Sect. 4, after the initial simulations and the calibration of the model, the

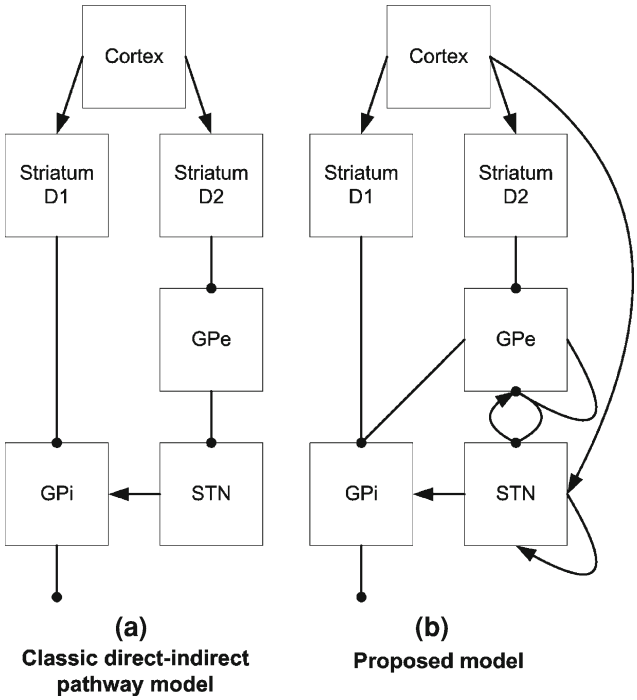

Fig. 4 **a** Box-and-arrow diagram of the classic direct–indirect pathway model of the basal ganglia. The various nuclei are depicted with *boxes* and their interconnections with *arrows* (*circle headed* and *arrow headed* for inhibitory and excitatory projections, respectively). The direct pathway is on the *left* (striatum D1 → GPi) and the indirect one on the *right* of the diagram (striatum D2 → GPe → STN → GPi). **b** Analogous box-and-arrow diagram of the population level model of the basal ganglia proposed in this study. Totally, there are five more connections than in the classic model: the loop-closing connection from the STN to the GPe, the two intranuclear connections within the GPe and the STN, the projection from the GPe to the GPi and the hyperdirect pathway from the cortex to the STN

$v_\mathrm{h}^\mathrm{GPe}$ and $v_\mathrm{h}^\mathrm{GPi}$ parameters are finally set to 14 and 12 mV, respectively.

With regard to the connectivity scheme of the model, apart from the classic direct–indirect model's pathways (Penney and Young 1983; Albin et al. 1989) and the cortical projection to both segments of the striatum, we have also incorporated the cortical projection to the STN (the so-called hyperdirect pathway; Nambu et al. 2002; Nambu 2005), the loop-closing connections between the GPe and the STN (Terman et al. 2002; Gillies and Willshaw 2004), the projection from the GPe to the GPi (Kita and Kitai 1991), and, finally, two internal projections within the GPe and the STN, respectively (Charara et al. 2003; Gillies and Willshaw 2004). A comparative diagram of the classic direct–indirect pathway model and the anatomical organization of the proposed model is shown in Fig. 4.

For simplicity, the values of the A_AMPA–D_AMPA, A_NMDA–D_NMDA and A_GABA–D_GABA parameters were the same for all the AMPA, NMDA, and GABA receptor H modules, respectively. Adapted to the equivalent PSP form of the pop-

Table 2 The parameters of the model and their normal baseline values

Parameters of the S modules (sigmoid functions of the populations)		
$S_{max}^{D1} = 300$ spikes/s	$k^{D1} = 0.3\,mV^{-1}$	$v_h^{D1} = 27$ mV
$S_{max}^{D2} = 300$ spikes/s	$k^{D2} = 0.3\,mV^{-1}$	$v_h^{D2} = 27$ mV
$S_{max}^{GPe} = 400$ spikes/s	$k^{GPe} = 0.2\,mV^{-1}$	$v_h^{GPe} = 14$ mV
$S_{max}^{GPi} = 300$ spikes/s	$k^{GPi} = 0.2\,mV^{-1}$	$v_h^{GPi} = 12$ mV
$S_{max}^{STN} = 500$ spikes/s	$k^{STN} = 0.2\,mV^{-1}$	$v_h^{STN} = 18.5$ mV
Parameters of the H modules (PSP forms elicited by synaptic receptor function)		
$A_{AMPA} = 2\,e$ mV		
$D_{AMPA} = 4^{-1}\,e\,ms^{-1}$		
$A_{NMDA} = 0.1\,e$ mV		
$D_{NMDA} = 100^{-1}\,e\,ms^{-1}$		
$A_{GABA} = 2\,e$ mV		
$D_{GABA} = 6^{-1}\,e\,ms^{-1}$		
Number of synaptic contacts in each connection (C parameters)		
$C^{CTX \to STR} = 50$	$C^{CTX \to STN} = 2$	$C^{D1 \to GPi} = 22$
$C^{D2 \to GPe} = 33$	$C^{GPe \to STN} = 10$	$C^{STN \to GPe} = 3$
$C^{GPe \to GPe} = 1$	$C^{STN \to STN} = 2$	$C^{GPe \to GPi} = 5$
$C^{STN \to GPi} = 3$		
Transmission delays		
$\tau^4 = \tau^{CTX \to STR} = 4$ ms	$\tau^3 = \tau^{STR \to GP} = 3$ ms	$\tau^1 = \tau^{other\ connections} = 1$ ms
Cortical firing parameters (Gaussian random process)		
Mean firing rate = 3 Hz	Variance = 1 Hz	

ulation level architecture (Eqs. 2, 3, and Fig. 3), the values used for the putative normal condition of the PSP parameters were $A_{AMPA} = 2\,e\,mV$, $D_{AMPA} = 4^{-1}\,e\,ms^{-1}$, $A_{NMDA} = 0.1\,e\,mV$, $D_{NMDA} = 100^{-1}\,e\,ms^{-1}$, $A_{GABA} = 2\,e\,mV$, and $D_{GABA} = 6^{-1}\,e\,ms^{-1}$. These values are generally thought to be representative of the mean normal receptor functioning, providing a good baseline approximation (Czubayko and Plenz 2002; Gerstner and Kistler 2002; Humphries et al. 2006).

For the selection of the values of the C parameters of the synaptic connections, we based our approach on the schematic drawings of the pattern of innervation of neurons of the GPe, the GPi and the STN originally presented in Shink and Smith (1995) and later modified in Charara et al. (2003). Those drawings incorporate the mean relative proportions of each type of synaptic contact to each neuron, as obtained by tracing studies in monkeys. For the GPe, there are 33 terminals from the striatal D2 segment (indirect pathway), three terminals from the STN (loop-closing connections between GPe and STN) and one terminal from intranuclear efferents. The GPi accepts 22 terminals from the D1 segment of the striatum (direct pathway), five terminals from the GPe, and three from the STN (indirect pathway). Finally, the STN receives input from 10 GPe-sourced contacts and two contacts by each of itself (intranuclear connectivity), cortex (hyperdirect pathway), thalamus, and pendunculopontine nucleus (which are excluded from the present model). All those observed numbers were the ones used in the model as the C parameters of the corresponding connections. For the cortical projection to striatum, we used—for either of the D1 and the D2 segments—a value of 50 synaptic contacts. This value is justified from reports about the location of corticostriatal buttons, found predominantly on the dendritic spines of the medium spiny neurons of striatum, and their number (Kincaid et al. 1998), compared to the respective numbers of the GPe targeting projections (Falls et al. 1983).

The values of the axonal delays of the connections were selected so as to satisfy the experimentally found propagation times through the pathways of the basal ganglia (van Albada and Robinson 2009). These are reported to be in the range of 8–11 ms for the early GPe excitation (cortex → STN → GPe), 15–19 ms for the GPe inhibition (cortex → D2 → GPe), and 26–32 ms for the late GPe excitation (cortex → D2 → GPe → STN → GPe). According to the analysis performed in van Albada and Robinson (2009), the propagation delays are given by the sum of all the axonal propagation delays in the considered pathway and all the dendritic and synaptic latencies of the populations that are found in the pathway. In our model, because of the nature of the population level formulation used, the dendritic and synaptic latencies are lumped into the synaptic time constants D (Table 2). Thus, the total propagation times can be found as the summation of all the axonal delays and the time constants D in the respective pathway. The values of the axonal delays used in van Albada and Robinson (2009) are 2 ms for the two cortex–striatum connections

and 1 ms for all the rest. For these axonal delay values and the synaptic time constants of Table 2, the cortex–STN–GPe pathway induces a delay of 1+4+1+4 ms [cortex–STN axonal delay + cortex–STN synaptic time constant(=AMPA time constant) + STN–GPe axonal delay + STN–GPe synaptic time constant(=AMPA time constant)] = 10 ms for the onset of the early GPe excitation. That lies within the expected range of 8–11 ms. Similarly, the inhibitory response of the GPe, induced by the cortex–striatum D2–GPe pathway, is delayed by 2+4+1+6=13 ms, while the expected range is 15–19 ms. In order to comply with the expected range, we selected increased values, in respect of the values used in van Albada and Robinson (2009), for the axonal delays between the cortex and the D2 striatal segment (=4 ms), on the one hand, and between the D2 striatal segment and the GPe (=3 ms), on the other hand. With these modifications, the propagation delay in the cortex–D2–GPe pathway of our model is 17 ms. For the second GPe excitation, induced by the striatum cortex–D2–GPe–STN–GPe pathway, considering the previously mentioned new delay values, the similar summation of axonal delays and synaptic time constants gives a delay of 4+4+3+6+1+6+1+4=29 ms, which is also in the middle of the expected range of 26–32 ms. Therefore, with our final selection of values for the axonal delays (summarized in Table 2), all the propagation delay times are in the middle of the expected ranges.

For the modeling of the cortical activity, a Gaussian random process was used. In this model, the cortex, i.e., the random process, provides input to both striatal segments and the STN. The mean cortical firing rate is reported to be around 3 Hz in normal rest states (Bauswein et al. 1989), and that is used as a mean for the Gaussian process, together with a variance of 1 Hz.

The proposed model is schematically depicted in detail in Fig. 5. Each excitatory connection affects its postsynaptic population by AMPA and NMDA receptor H modules and each inhibitory by GABA receptor modules. From the 17 H modules of the proposed model, 34 first-order differential equations of the type of (4) are derived.

According to the model's architecture (Fig. 5) and (5), the LFP of the STN was obtained by the equation:

$$\begin{aligned} v_{\mathrm{STN}} = {} & {H_{\mathrm{AMPA}}}^{\mathrm{CTX}} + {H_{\mathrm{NMDA}}}^{\mathrm{CTX}} \\ & + {H_{\mathrm{AMPA}}}^{\mathrm{STN}} + {H_{\mathrm{NMDA}}}^{\mathrm{STN}} \\ & - {H_{\mathrm{GABA}}}^{\mathrm{GPe}} \end{aligned} \tag{7}$$

where the superscript of each H module denotes the source population.

The model's set of equations was solved using the 4th order Runge–Kutta method for a 10-s period with 3-kHz sampling rate. Every simulation was also performed by solving the equations with other numerical algorithms, such as the Bogacki–Sampine and the Dormand–Prince, and different sampling rates (3–10 kHz), to support the validity of the results.

The normal rest state operating condition of the model was replicated by using the values for the parameters of the populations and their synaptic connectivity, which have already been presented so far and are summarized in Table 2. The evaluation of the normal behavior of the model was based on the definition of the target expressions of such a condition, as reported in the literature. In terms of the firing rate activity of the nuclei, we defined as target firing rates those used in Humphries et al. (2006): $S^{\mathrm{STN}}_{\mathrm{normal}} = 9.3 \pm 0.8$ spikes/s, $S^{\mathrm{GPe}}_{\mathrm{normal}} = 31.2 \pm 2.2$ spikes/s, and $S^{\mathrm{GPi}}_{\mathrm{normal}} = 28.1 \pm 2.27$ spikes/s. For both striatal segments, the firing rates in normal rest state condition are expected to be very low, near zero, reflecting the quiescent nature of the striatum in the absence of strong, synchronized cortical input. In addition to the firing rates, the PSD function of the STN's LFP in the normal rest state condition is expected to be similar to the experimentally recorded ones, reported in Brown et al. (2002) and Sharott et al. (2005).

3.3 Parkinsonian behavior of the model

As briefly discussed in Sect. 1, the alterations that take place in the parkinsonian condition as a consequence of the lack of dopamine are related to the strengths of the synaptic connections between the nuclei. In the proposed model, the strengths can be adjusted either by the modification of the number of physical synaptic contacts between populations (C parameters) or by the modification of the PSPs elicited by synaptic activity. According to the presently known facts about PD, the former is not a plausible possibility, and, hence, it is not considered here. On the contrary, the latter is well supported by experimental studies of dopamine-depleted states, as mentioned in the introduction. Also, the transmission delays of the synaptic connections are considered to be defined by the signal conduction characteristics of the axons, and no change to them is expected by dopamine depletion. All the other time dependencies in the synaptic pathways are concentrated in the time constants of the PSPs.

In general, the PSPs are differently modulated by the two main dopamine receptor classes, the D1 and D2 families. Although the functioning of dopamine receptors is quite complicated (Missale et al. 1998), we can generally consider that D1-/D2-class receptors enhance/decrease PSPs in high dopamine concentrations (Seamans and Durstewitz 2008). In cases of dopamine depletion, such as in PD, D1 receptor's activation is decreased, and so the enhancement is lower; D2 receptor's activation is also decreased, and so the reduction is also lower. Their effects oppose—with D1 class pointing to dampened PSPs, and D2 class to strengthened ones. Apart from a clear distinction between the D1 and D2 regions of striatum where only one type of receptor is thought to be

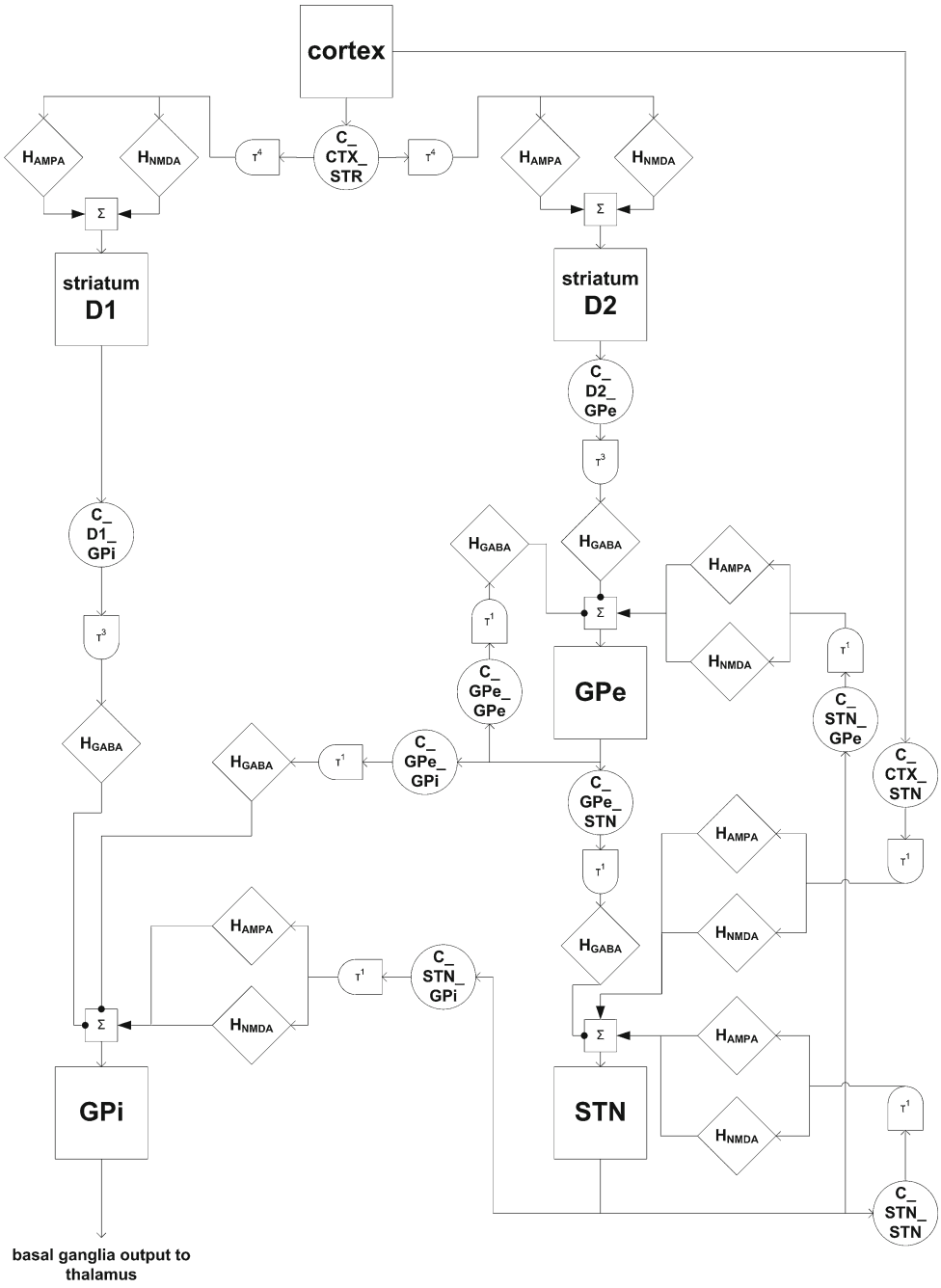

Fig. 5 The proposed model of the basal ganglia constructed according to the population level architectural scheme presented in Fig. 2 and following the box-and-arrow diagram of Fig. 4b. Each *square box* (*S* module) encapsulates a sigmoid function with three parameters, apart from the cortex which is modeled as a Gaussian random process. Each *diamond* (*H* module) represents the PSP contribution of one particular type of neurotransmitter. AMPA and NMDA are used for excitatory connections, and GABA is used for inhibitory ones. Each *H* module corresponds to a set of two first-order differential equations of the form of equation (4), with two parameters. Each circle describes the mean number of physical synaptic contacts between populations. The transmission delays τ^1, τ^3, and τ^4 correspond to the respective parameters presented in Table 2

expressed in each, all the other nuclei of the basal ganglia co-express the two classes (Beckstead et al. 1988; Kreiss et al. 1997; Baufreton et al. 2005). Thus, the PSPs elicited to the populations of the model by each connection might be either strengthened or weakened in abnormal conditions, depending on the particular type of dopamine receptor that controls the modulation.

However, published experimental studies have provided specific data about the actual modulations, indicating that in dopamine- depleted states, the connections to the STN from itself, the cortex, and the GPe are strengthened (Shen and Johnson 2000; Shen et al. 2003; Floran et al. 2004), as are also the projections of the striatal D2 segment and the STN to the GPe (Johnson and Napier 1997; Cooper and Stanford 2001). All these connections are, therefore, thought to be modulated by D2 dopamine receptors. The cortical input to the striatum is mediated not only by D2 receptors in the D2 segment, but also by D1 receptors in the D1 segment. Thus, these connections are enhanced and weakened, respectively, in PD (West and Grace 2002). On the contrary, the intra-GPe connections are expected to remain unaltered (Cooper and Stanford 2001). Finally, the striatal afferent to the GPi is

modulated by the D1 receptor type, whereas the GPe → GPi and STN → GPi connections are most likely mediated by the D2 receptor type (Johnson and Napier 1997; Lange et al. 1997).

Far from the synaptic connections, specific quantitative trends for the alterations of the intrinsic firing properties of the nuclei of the basal ganglia under dopamine depletion have not been established, and they are, therefore, not considered in the present modeling study. Although some studies have reported changes in the functionality of neurons elicited by altered dopaminergic modulation (Yasumoto et al. 2002), dopamine is mainly considered a synaptic modulator that does not induce immediate changes to neuronal activities, but rather affects them through its influence to the action of other neurotransmitters (Barchas et al. 1978).

Based on all the above facts about the expected alterations of the basal ganglia in PD and the hypothesis that the time course of the PSPs may play a role in the pathophysiological synchronization of the system, we replicated the parkinsonian condition by modifying the A and D parameters of the H receptor modules of all connections, i.e., the A_{AMPA}, D_{AMPA}, A_{NMDA}, D_{NMDA}, A_{GABA}, and D_{GABA} parameters. The actual percentage of modification of these parameters is not precisely known. Several experimental studies have presented data about the amount of modification of the amplitude of PSPs within minutes or hours of the initiation of the dopamine depletion (Calabresi et al. 2000; Bamford et al. 2004). However, in chronic dopamine depletion, where the pathogenic condition lasts for years, the modifications may be different. Also, owing to the lack of specific quantitative data about the exerted alterations of dopamine depletion to each and every connection in the basal ganglia, we treated them all the same, by inserting two universal variables that control the percentage of the modification of the PSPs of all the synaptic connections. The amplitudes of the PSPs are modified by a factor α, and the time constants by a factor δ. If a connection is mediated by D2 dopamine receptors, and is, therefore, strengthened in PD, then both factors are used to multiply the normal amplitudes and time constants. Alternatively, if a connection is D1-mediated, being weakened in PD, then the same factors are used to divide the normal values. The minimum value for α and δ is 1 and corresponds to the normal condition.

In order to reach conclusions about the critical pathophysiological alterations that lead to the appearance of the PD signs, we explored the behavior of the model for all the combinations of values for the α and δ parameters, in the 1–6 range for each, with a step of 0.02. The exploration was performed without taking a priori into account the available knowledge about the alterations of the synaptic connections in dopamine-depleted states. For each connection, we considered three possibilities in PD: enhancement (modulation controlled by D2 dopamine receptors), weakening (modulation controlled by D1 dopamine receptors) or no change. These are described by inserting for each connection a p parameter that can be independently set to 1, −1 or 0, respectively. Therefore, the pathological amplitudes and time constants are given in relation to the normal ones (Table 2) by the following equations:

$$A^{s\to t}_{\mathrm{R,path.}} = A_{\mathrm{R,normal}} \cdot \alpha^{p^{\mathrm{s}\to\mathrm{t}}} \tag{8a}$$

$$D^{s\to t}_{\mathrm{R,path.}} = D_{\mathrm{R,normal}} \cdot \delta^{p^{\mathrm{s}\to\mathrm{t}}} \tag{8b}$$

where R: {AMPA, GABA, or NMDA}. The s → t (source → target) notation represents all the synaptic connections included in the model, i.e., CTX → D1, CTX → D2, CTX → STN, D1 → GPi, D2 → GPe, GPe → STN, STN → GPe, GPe → GPe, STN → STN, GPe → GPi, and STN → GPi.

In the exploration, the parkinsonian behavior of the model was identified by the emergence of a beta band spectral peak in the PSD function of the STN's LFPs. Since the connections targeting the GPi, i.e., the direct pathway (CTX → striatal D1 and D1 → GPi), the STN → GPi, and the GPe → GPi, only affect the GPi's firing rate and not the STN's LFPs, we eliminated them from the exploration, to reduce the number of cases that needed to be explored (from 3^{11} to 3^7).

After the end of the exploration and having gathered the cases and the $\{\alpha, \delta\}$ values that produced a beta band peak, we evaluated the plausibility of the putative parkinsonian condition of the model by checking the mean firing rates of the nuclei. The expected values cannot be precisely constrained (there are plenty of contradicting reports in the literature), but rather qualitatively assessed by their relations to the corresponding normal rates. Thus, based on known facts about PD pathophysiology, we expected increased firing for the striatal D2 segment, the STN, and the GPi, and decreased firing for the D1 striatal segment and the GPe.

Far from the beta band, it has been reported recently that synchronizations in other frequency bands may be present in LFP recordings from parkinsonian subjects (Priori et al. 2004; Kühn et al. 2008). Such an observation is also supported in part by our recordings (as mentioned in the Material section): The characteristic peaks in the PSD functions of the LFP recordings of two subjects were above the theoretical boundaries of the beta band. Although the boundaries of the bands cannot be strictly defined, the establishment of the significance of frequencies outside the beta band in PD would be very interesting. In this study, after having determined the necessary alterations for the model generation of the beta band, we investigated whether the same types of alterations could lead to synchronization in other frequency bands, as well. The investigation was performed by a similar exploration as for the beta band, but with a wider range of frequencies within which we searched for spectral peaks or increased energies.

4 Results

The initial simulation of the model with the baseline normal configuration of parameters (Table 2) yielded the following mean firing rates for the populations: $S^{D1}_{mean} = 0.2$ spikes/s, $S^{D2}_{mean} = 0.2$ spikes/s, $S^{STN}_{mean} = 4.4$ spikes/s, $S^{GPe}_{mean} = 44.6$ spikes/s, and $S^{GPi}_{mean} = 22.8$ spikes/s. All the standard deviations were very small. The deviation of these initial simulation results from the targets for the STN, GPe, and GPi populations is expected because the model is not properly calibrated. In order to approach the targets, we adjusted the v_h parameters of GPe and GPi. That is actually similar to the calibrations performed in the modeling study of Humphries et al. (2006), where the intrinsic currents of the neurons are properly selected. There is one constraint, though, since the adjustment of the v_h parameters affects the intrinsically invoked firing rates of the populations [the $S(0)$ value of (6)]. The plausible range is 2–30 Hz for the GPi (Nakanishi et al. 1990) and 2–40 Hz for the GPe (Kita and Kitai 1991). The final selection of the values of the v_h parameters was such that it did not violate these ranges: $v_h^{GPe} = 14$ mV ($S(0)^{GPe} = 22.5$ spikes/s), and $v_h^{GPi} = 12$ mV ($S(0)^{GPi} = 24.5$ spikes/s).

After the adjustments, the simulated normal rest state yields mean firing rates: $S^{D1}_{mean} = 0.2$ spikes/s, $S^{D2}_{mean} = 0.2$ spikes/s, $S^{STN}_{mean} = 7.5$ spikes/s, $S^{GPe}_{mean} = 23.1$ spikes/s, and $S^{GPi}_{mean} = 20.6$ spikes/s, all with small standard deviations. Some deviation from the target rates remains, but we consider the achieved rates acceptable. Subsequently, we kept the selected values for the v_h^{GPe} and v_h^{GPi} parameters unchanged for the simulation of the parkinsonian condition.

The model-derived LFP of the STN in the normal rest state condition is depicted in Fig. 6, in both time and frequency domains. The exhibited patterns of the traces in both domains are consistent with the experimentally recorded ones (Brown et al. 2002; Sharott et al. 2005). In particular, the characteristic elevation of the PSD function in the low frequencies is reproduced by the model as a result of the contribution of the NMDA currents.

After having established the validity of the model's behavior in the normal condition, we proceeded in the exploration of the pathophysiological behavior of the model. Through the exploration, we searched for configurations that resulted in the expression of a beta band peak in the PSD function of the STN's LFP and in PD-plausible firing rates of all the nuclei. The exploration was performed once, combining the p, α, and δ parameters: for each set of p parameter values, the output of the model for all the combinations of values for α and δ in the range 1–6 with step 0.02 was evaluated. A peak was detected based on the relative concentration of energy in the beta band.

Regarding the point of the spectral peak in the beta band, it has been observed from the available real recordings that, for each subject, all the recordings that include a dominant beta band peak in their PSDs have that peak at the same frequency point. Thus, there is one specific frequency point of the beta band for each subject. That may be distinct across subjects. This observation, if established, may lead to the consideration of the frequency point of the beta peak as an individualized characteristic. Such a property of the beta peak would indicate that it may carry specific information about the pathophysiological hallmarks of PD, such as personalized or disease's stage characteristics.

In the discussion hereafter, we will not strictly use the actual LFP signals either in time or frequency domains, but we will try to capture the above described property of the beta peak by the model and assign its root cause to specific functional parameters. For this purpose, the design and the analysis of the results of the simulations were largely based on the above property.

The exploration of the pathophysiological behavior of the model showed that out of the 3^7 cases explored (the number of the different sets of p parameter values) the model exhibited a beta band peak only for the following two general sets of p values for the synaptic connections:

$$\begin{aligned}
&\text{PD-case I: } p^{CTX\to D2} = 1,\ p^{CTX\to STN} = *,\\
&\quad p^{D2\to GPe} = 0,\ p^{GPe\to STN} = 1,\ p^{STN\to GPe} = 1,\\
&\quad p^{GPe\to GPe} = *,\ p^{STN\to STN} = 1\\
&\text{PD-case II: } p^{CTX\to D2} = 1,\ p^{CTX\to STN} = *,\\
&\quad p^{D2\to GPe} = 1,\ p^{GPe\to STN} = 1,\ p^{STN\to GPe} = 1,\\
&\quad p^{GPe\to GPe} = *,\ p^{STN\to STN} = 1
\end{aligned}$$

The '*' symbol for the $p^{CTX\to STN}$ and $p^{GPe\to GPe}$ parameters denotes that all the possible combinations of their values appear in the set of PD-cases I and II.

The behavior of the model regarding the presence and the specific point in the beta range of frequencies of the beta band peak was similar in all the combinations of possible values for the $p^{CTX\to STN}$ and $p^{GPe\to GPe}$ parameters for both PD-cases I and II. This suggests that the beta synchronization is independent of the CTX → STN and GPe → GPe connections. Thus, we are now going to present the exhibited behavior of the model only for the representative PD-cases I and II. Pathophysiologically, the difference between them lies only in the state of the D2 → GPe connection, being unaltered and enhanced, respectively, as a result of the dopamine depletion. Figure 7 shows the beta band peak maps obtained by the exploration, which summarize the dependence of the point of the beta band peak in frequencies on the $\{\alpha, \delta\}$ couples in each of the two cases.

The firing rates of the nuclei in both cases depend on the $p^{CTX\to STN}$ and $p^{GPe\to GPe}$ parameters. Also, GPi's firing rate is affected by the state of the four connections that we did not consider in the explorations, i.e., the parameters

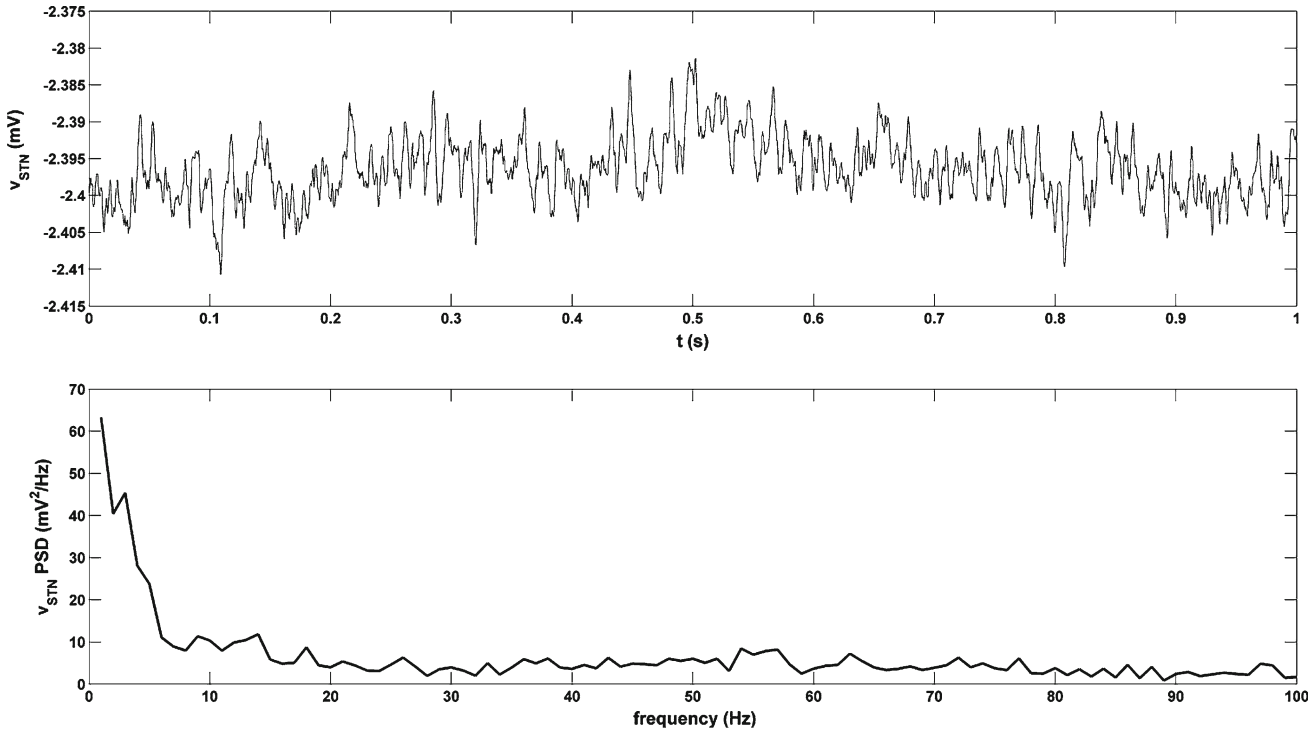

Fig. 6 The model generated STN's LFP signal in the normal condition. *Above*: the temporal form of the LFP signal for a sample 1 s is shown. *Below*: the PSD function of the LFP signal is presented in the 0–100 Hz range

$p^{\mathrm{CTX}\to\mathrm{D1}}$, $p^{\mathrm{D1}\to\mathrm{GPi}}$, $p^{\mathrm{GPe}\to\mathrm{GPi}}$ and $p^{\mathrm{STN}\to\mathrm{GPi}}$. According to the available experimental data (West and Grace 2002; Shen and Johnson 2000; Shen et al. 2003; Floran et al. 2004; Cooper and Stanford 2001; Johnson and Napier 1997), it is expected that $p^{\mathrm{CTX}\to\mathrm{STN}} = 1$, $p^{\mathrm{GPe}\to GPe} = 0$, $p^{\mathrm{CTX}\to\mathrm{D1}} = -1$, $p^{\mathrm{D1}\to\mathrm{GPi}} = -1$, $p^{\mathrm{GPe}\to\mathrm{GPi}} = 1$ and $p^{\mathrm{STN}\to\mathrm{GPi}} = 1$, and so, these are the values that we finally used for the extraction of the firing rates.

The couples of mean $\{\alpha, \delta\}$ values, for which a beta peak emerged, and the firing rates were PD-plausible (according to the rules referred in Sect. 3), versus the specific point of the peak in the beta band are plotted in Fig. 8. Figure 9 presents the percentage of change of the PSP integrals, while Fig. 10 presents the mean firing rates of all the populations for these $\{\alpha, \delta\}$ couples. Also, Table 3 contains overall the mean firing rates of the populations in the parkinsonian condition, for each of the two PD-cases.

Finally, Fig. 11 presents an example of the temporal evolution of the output firing rates of the GPe and the STN, along with the exhibited beta band peak. As revealed by the plot, this characteristic beta band peak is a consequence of the intense, synchronized oscillations of the GPe–STN network. The beta frequency was produced by the specific time period of transitions between intense and quiescent activity. The emergence of the oscillations itself is the result of the enhancement of the inhibitory input to the GPe along with the enhancement of the excitatory input to the STN. The closed GPe–STN loop would not have been driven to oscillations if a certain amount of inhibition to the GPe and excitation to the STN would not have been reached. These amounts are determined by the integrals of the PSPs (Fig. 9).

The model suggests that the cascade of events leading to the initiation and the sustentation of the oscillatory activity is as follows:

(1) Owing to the enhanced cortical input to the striatum, its D2 segment turns hyperactive.
(2) The increased inhibition of the D2 segment to the GPe forces the latter nucleus to fire less on average.
(3) The shutting of GPe unlooses STN, which goes to a fast firing pace.
(4) Since STN is excitatory to GPe, and as the influence of the former on the latter is greatly strengthened due to the parkinsonian synaptic alterations, GPe starts to fire more and reaches a high level of firing activity.
(5) Since GPe is inhibitory to STN, and as the influence of the former on the latter is also greatly strengthened due to the parkinsonian synaptic alterations, GPe strongly inhibits STN, which falls to low firing rates.
(6) The tight interplay between GPe and STN, along with their constant external driving from the striatal D2 segment and the cortex, respectively, results in the preservation of the iterations of the steps (4) and (5). The specific period of these iterations produce the

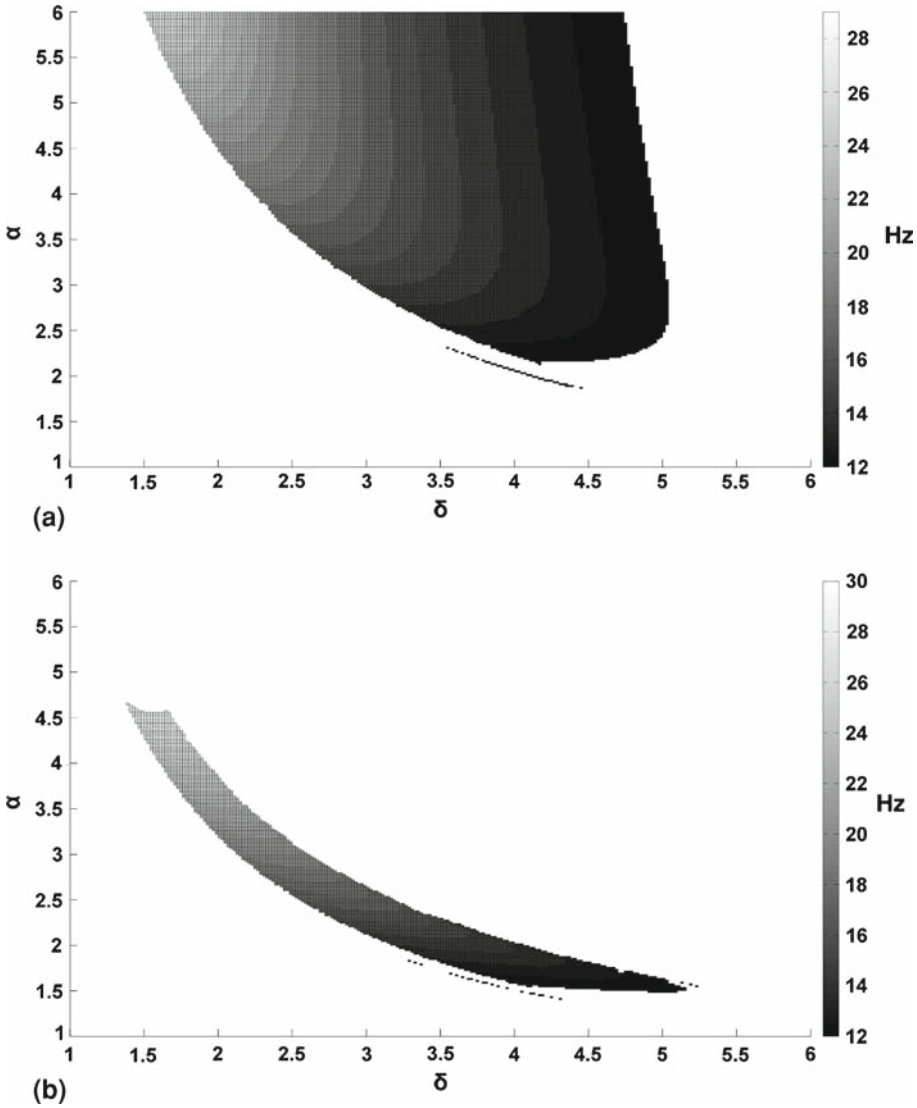

Fig. 7 The beta band peak appearance maps obtained from the explorations of the model's behavior for all the combinations of $\{\alpha, \delta\}$ values in the range 1–6 for each, with a step of 0.02, for both PD-cases, **a** I and **b** II. For both cases, high beta peaks are obtained by low δ values and the reverse

characteristic peak and its point in frequencies is determined by the values of the synaptic time constants in association with the axonal delays, in the GPe–STN network.

Figures 10 and 11 also suggest that the intensity of the firing of the nuclei does not affect the presence of the peak and its point in the beta band. That is why the firing rates of the nuclei produced for some $\{\alpha, \delta\}$ couples are implausible, despite the emergence of a beta peak for those couples.

The exploration for dominant rhythms in other frequency bands, outside the beta, resulted in a wide range of exhibited energy distributions in the PSD function of the STN's LFPs generated by the model. Out of them, four main patterns emerged, which are presented in Fig. 12. The different patterns were a result of changes in the values of the parameters α and δ. Thus, it is suggested that solely the dopaminergic modulation of both the amplitude and the time course of the PSPs may lead not only to the emergence of the characteristic beta band, but also to other forms of dynamical behavior of the basal ganglia, as well.

5 Discussion

The proposed population level computational model of the basal ganglia suggests that it is the dopamine-depletion-triggered modification of both the amplitude and the time course of the PSPs, which leads to the appearance of the main parkinsonian expression, the characteristic beta band peak in the PSD function of the STN's LFP signals. Thus, not only is it indicated that the dual synaptic modulation is of pivotal importance in the physiology of the system, but it is also shown that the time course of the PSPs does, in fact, play a significant role in its physiology. Experimentally, the dependence of the PSP time course on dopamine concentration

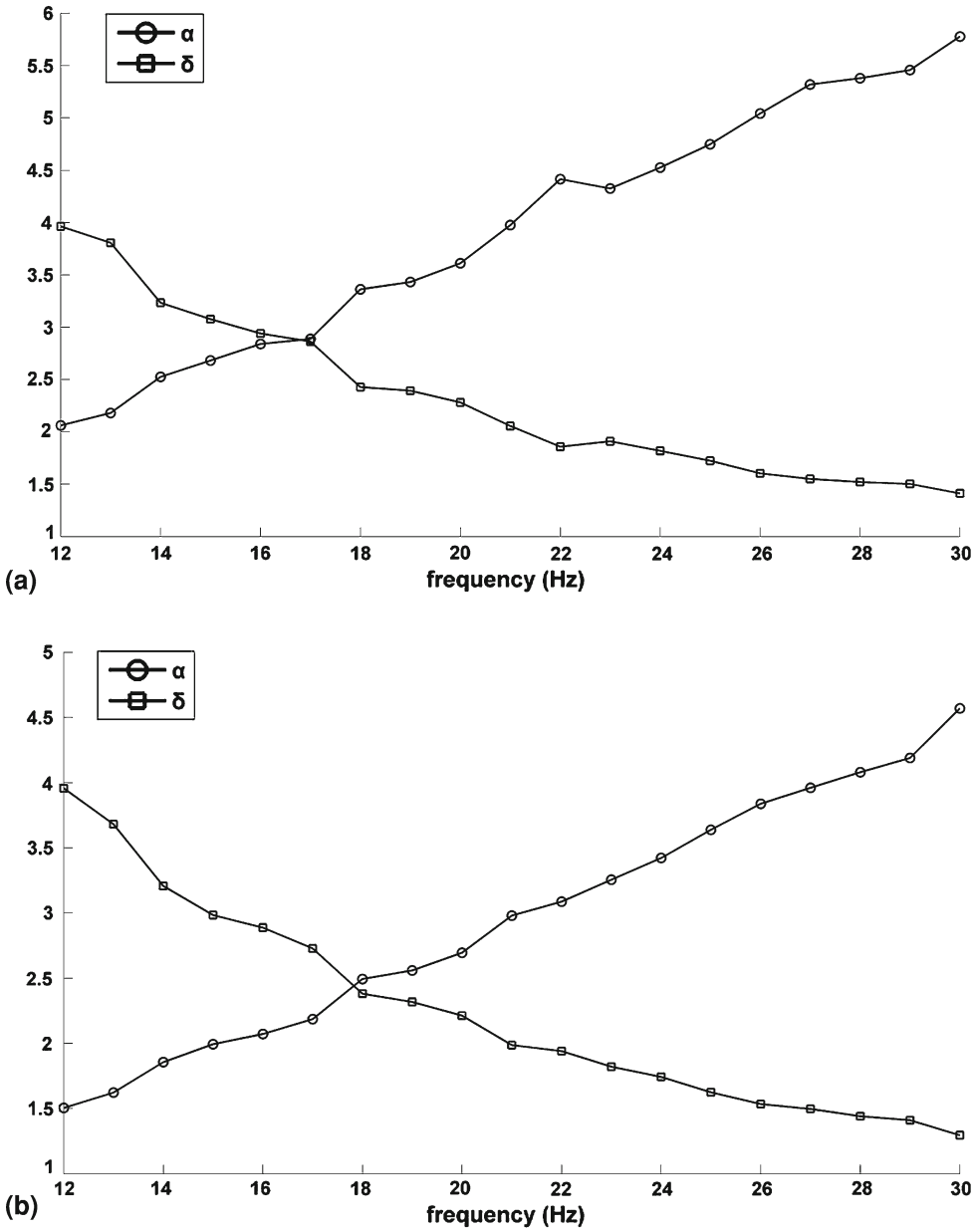

Fig. 8 The sets of mean $\{\alpha, \delta\}$ couple values for the expression of the beta band peak in the various frequency points in the beta range (12–30 Hz). For both cases, the emerging patterns dictate the inverse relation of α and δ to the beta band peak point

has not been demonstrated yet. However, most of the experimental studies that examined the alterations induced by the altered dopaminergic concentration only dealt with an isolated tissue within hours from the initiation of the depletion. In PD, the dopamine depletion lasts for years before giving actual symptoms. Therefore, we think that the current experimental limitations in space and time might obscure the exact effects of dopamine depletion. In this study, we anticipate specific dominant long-term effects of dopamine depletion related only to the amplitude and time course of the PSPs. The simulation results indicate that those alterations are sufficient for leading to the main expressions of PD. The establishment of the validity of this hypothesis for basal ganglia may lead to new insights, since the time course factor has not received much attention so far. This observation could be of importance for other brain systems, as well.

Through the simulations of the model, it is shown that the beta band peak reflects an abnormal oscillatory synchronization. That is in agreement with other studies (Boraud et al. 2005; Hammond et al. 2007). In particular, the model exhibits this peak when both the amplitude and the time course of the PSPs are driven to the putative pathophysiological range of values, leading to severe modification of the synaptic influences to the postsynaptic targets. In that condition, the model reveals that the GPe and the STN are mutually locked in intense synchronized oscillations. Then, both go from short periods of quiescent activity to short periods of intense activity and back. The beta band peak of the STN's

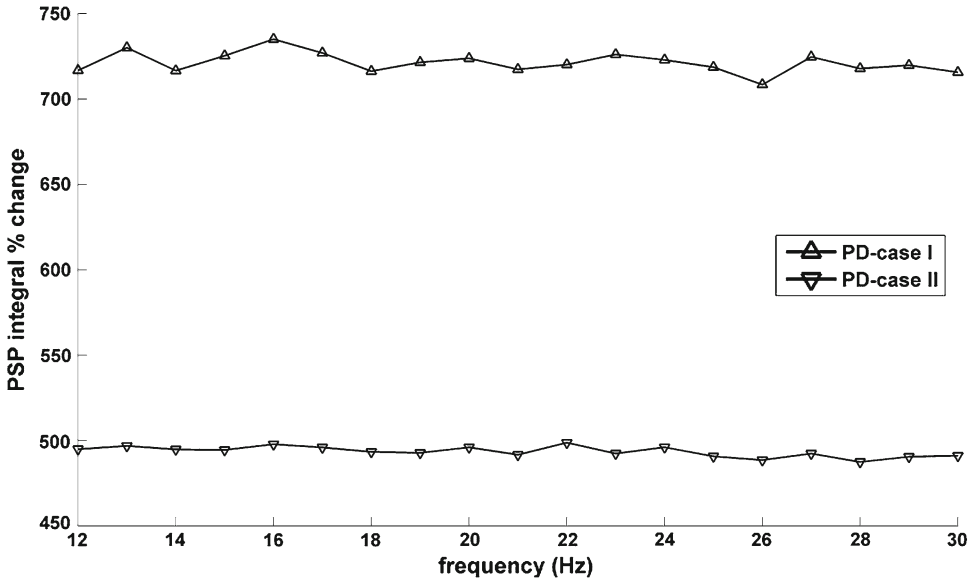

Fig. 9 The percentage of the synaptic strength change in PD-cases I and II, as a function of the frequency of the beta peak, calculated as the integral of the PSPs in the parkinsonian condition in relation to the normal PSPs. For the formation of the Parkinsonian PSPs, the respective values of α and δ from Fig. 8 were used. The inverse dopaminergic modulation of the amplitudes and time courses, as revealed in Fig. 8, results in an almost constant synaptic strength for both cases in all the beta frequencies

LFPs is then produced by the specific period of the oscillations. The latter is actually determined by the time constants of the synaptic connections and the transmission delays. In general, the emergence of the oscillations is a consequence of the combined enhancement of the total inhibitory afferent activity to the GPe and the total excitatory afferent activity to the STN. These results indicate that the beta synchronization is not transferred to the basal ganglia and the STN, in particular, from the cortex. Rather, it is implied that the pathological synchronization is produced within the basal ganglia as a result of the tight interplay of the GPe and the STN, in their characteristic closed loop. That is also consistent with previous modeling results (Bevan et al. 2002; Terman et al. 2002).

The exploration of the model's behavior for all the combinations of $\{\alpha, \delta\}$ values revealed that the characteristic parkinsonian beta band peak is reproduced if and only if both the loop closing connections between the STN and the GPe are mediated by D2 dopamine receptors, being enhanced under dopamine depletion. The same must be also the case for the cortical projection to the striatum's D2 neurons. The inhibitory projection of the latter to the GPe is shown to be either unaltered (PD-case I) or enhanced (PD-case II) for the model to exhibit a beta peak. However, the overall mean firing rates of the populations support better the latter case, mostly because the mean rate of the D2 striatal population turns out to be rather implausibly high in PD-case I. The model also predicts that the emergence and the specific point in frequency of the beta band peak are independent from the intranuclear GPe connection and the cortical projection to the STN. All these results are consistent with published data about the state of the synaptic connections under dopamine depletion, as presented in the introduction (West and Grace 2002; Shen and Johnson 2000; Shen et al. 2003; Floran et al. 2004; Cooper and Stanford 2001; Johnson and Napier 1997). More importantly, all these plausible synaptic alterations were finally captured by the model after performing an exploration through all the possible cases, without a priori assumptions.

In addition, the model predicted that the STN's intranuclear connection has to be enhanced for the emergence of the beta band peak. Through such a state for this connection, the STN receives increased excitation, which is necessary to sustain the synchronization of the STN–GPe loop. It must be noted that the existence of such a connection is a controversial feature of the network of the basal ganglia. Many experimental studies have not reported evidence about its presence (Sato et al. 2000), whereas several modeling studies have not considered it in their anatomical arrangements (Gurney et al. 2001; Terman et al. 2002). Other studies, however, argue for its existence (Charara et al. 2003; Gillies and Willshaw 2004; Shen and Johnson 2006). In any case, the point made by the model is that the STN must receive enhanced excitation in the parkinsonian condition to sustain the intense interplay with the GPe. The source of the excitation may not be necessarily the STN itself. Since also the cortical input may not be adequate to provide the needed amount of excitation, other sources may be possible, such as the thalamus or the pendunculopontine nucleus (Orieux et al. 2000). Both these nuclei are certain to excitatorily affect the STN. Thus, the existence or not of the STN intranuclear connections is not expected to affect the main conclusions of the present study.

Far from the beta band, the model holds the ability to produce LFP signals from the STN with dominant rhythmic activities in the alpha and gamma bands, as well. Depending on the values of the α and δ parameters of the dopaminergic modulation of the synaptic activity, either clear, sharp peaks or multiple rhythms may emerge. The transitions between

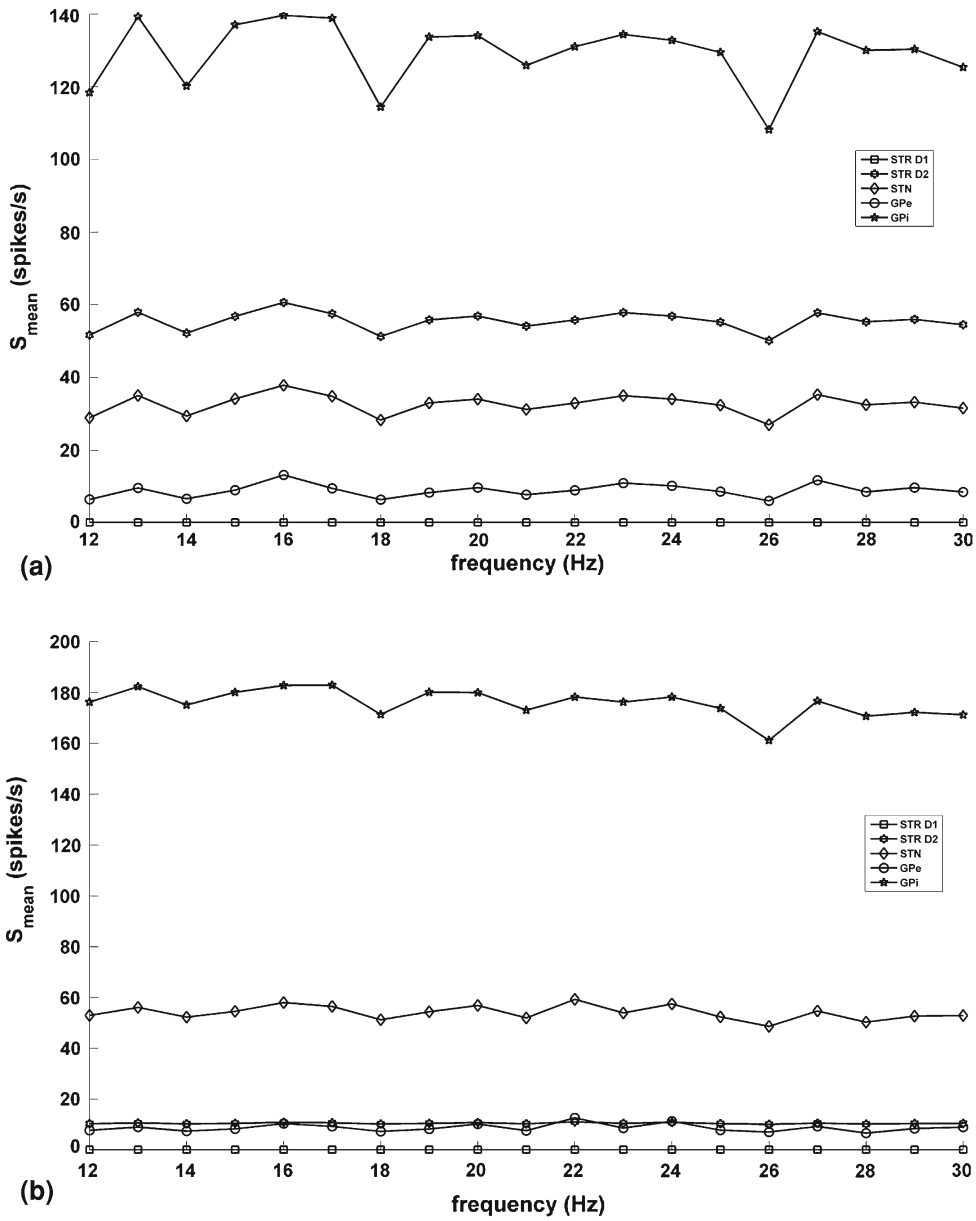

Fig. 10 The mean firing rates of all the populations of the model, as derived by using the sets of mean $\{\alpha, \delta\}$ values (shown in Fig. 8) for the expression of the beta band peak in the various frequency points in the range of 12–30 Hz, for PD-case **a** I, **b** II. The rates fluctuate around the same mean values for all the points of the beta band peak, indicating that the latter do not affect the mean firing levels of the nuclei

Table 3 The overall mean firing rates of the nuclei in each of the two PD-cases for which the beta band peak is reproduced

	PD-case I	PD-case II
Striatum D1	0.1 ± 0.01	0.1 ± 0.001
Striatum D2	55.5 ± 2.7	10.5 ± 0.3
STN	32.7 ± 2.7	54 ± 2.8
GPe	8.9 ± 1.9	8.8 ± 1.5
GPi	129.4 ± 8.7	175.9 ± 5.3

All the numbers have units of spikes/s

the different bands and rhythmic patterns depend solely on the α and δ parameters, indicating that these are the critical universal rhythmogenic factors in the basal ganglia.

In what concerns the relative amount of modification of the synaptic parameters, the results greatly depend on the selection of their normal baseline values. These cannot be in any terms unequivocally constrained, since there is actually a wide normal range of values. Though, the parametric calibration of this particular model leads to normal-like activities when the synaptic parameters take the values defined in the

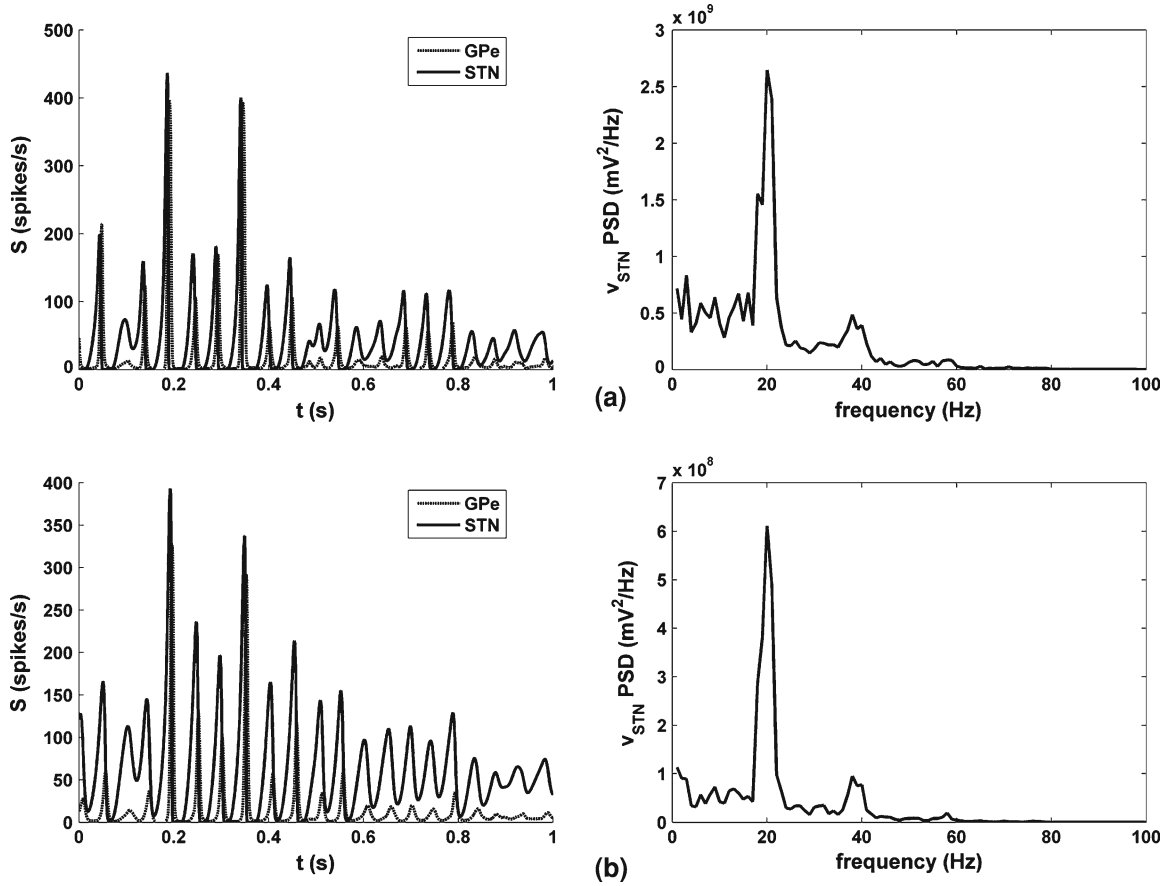

Fig. 11 A snapshot of the temporal firing rate outputs of the GPe and the STN populations during a sample 1 s (similar for all the simulated 10 s), for the two PD-cases that exhibited a beta band peak, **a** I and **b**: II. The two nuclei exhibit sharp transitions in their output firing rates, moving from short periods of intense-to-short periods of quiescent activity (plots on the *left*). The frequency of the oscillatory synchronization falls in the beta band, causing the characteristic peak to emerge (plots on the *right*)

reported used normal configuration (Table 2). That uniquely defines the comparative reference for the parkinsonian condition. From the explorations, the prediction that the modifications of the amplitudes and the time courses are, respectively, proportional and inversely proportional to the point of the peak in the beta frequencies turns out. In the future, this prediction may lead to indications toward the establishment of the specific effects of the dopaminergic modulation on the synaptic parameters. The results also reveal that, in the parkinsonian condition, the integrals of the PSPs were almost constant for all the frequency points of the beta peak. That indicates, on the one hand, that a specific amount of PSP strength is needed for the parkinsonian condition. On the other hand, it makes evident that the pathophysiological expressions in PD cannot be explained just by a simple modification of the synaptic strength; the qualitative and quantitative roles of both the amplitude and the time course of the PSPs are necessary.

Small perturbations of the values of the C and the sigmoid parameters do not affect the sets of $\{\alpha, \delta\}$ points for which the beta peaks emerge at specific points in frequency. On the contrary, the dependence of the mean firing rates of the nuclei on those parameters is inevitably strong, as their evaluation is determined by the basic assumptions of the population level architecture itself.

Considering further the simplifications and limitations of the presented approach, first and foremost, the population level architecture used by the model is itself a simplified paradigm. The representation of complex physiological interactions by simple mathematical functions with a few parameters can only provide a crude abstraction of the reality. Despite that, such simplifications are to a certain point inevitable when dealing with systems such as the basal ganglia, with so many nuclei, network interactions, and neuronal types. Along with the above, the goals of this study were thought to be adequately served by the population level approach. Far from the architectural simplifications, the selection of the values of the model's parameters suffers from the disparity of published data sources and the heterogeneity of the experimental conditions. The above

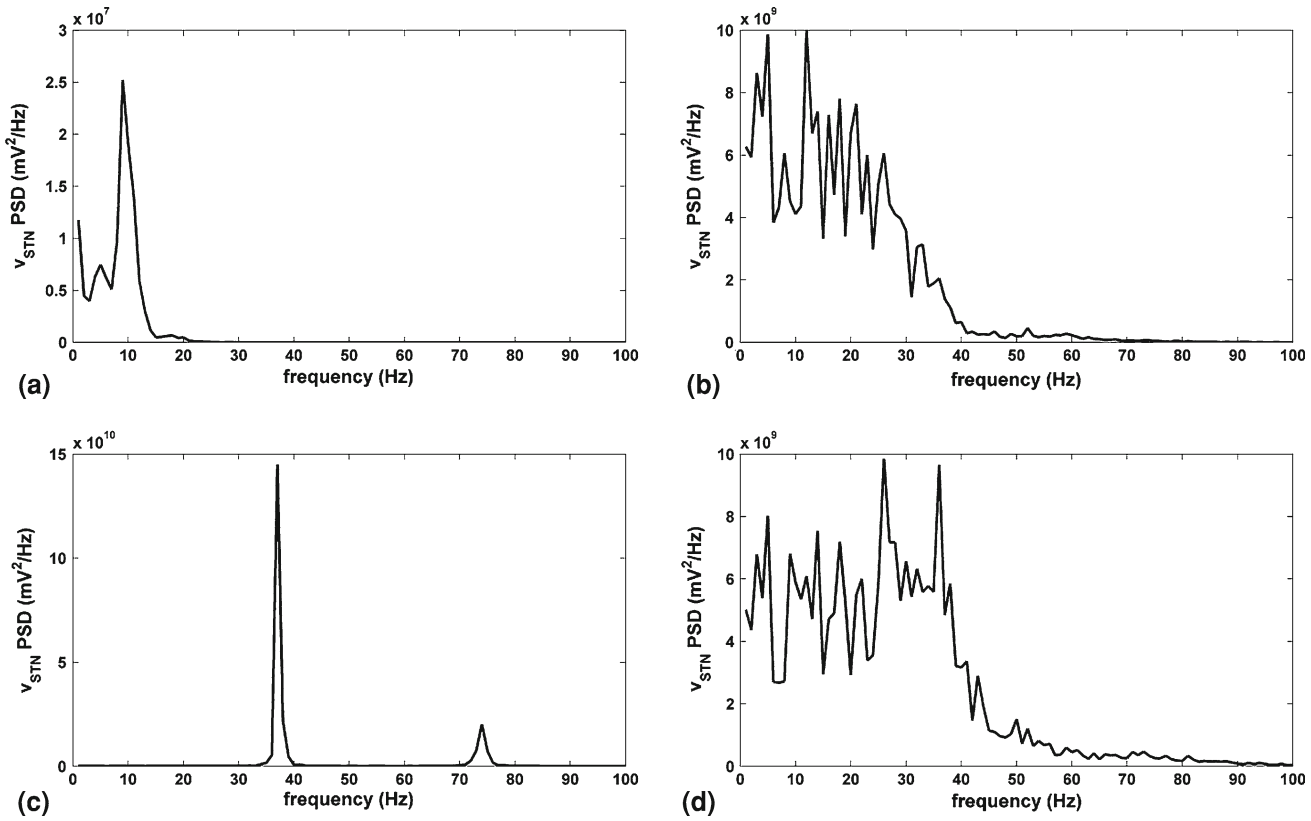

Fig. 12 Apart from the prominent beta band peak, the model can also generate LFP signals that are dominated by alpha or gamma rhythms. Here, the four main identified patterns for such rhythms are shown, only for PD-case II, for the parametric values: **a** $\alpha = 1.22$, $\delta = 4.82$; **b** $\alpha = 4.26$, $\delta = 1.96$; **c** $\alpha = 5.82$, $\delta = 1.2$; and **d** $\alpha = 5.9$, $\delta = 1.4$. In PD-case I, similar results are obtained, with the exception of the inability of the model to reach gamma frequencies above 33 Hz. The plots indicate that solely the changes of the PSP parameters are adequate for the generation of rhythmic activities in all the frequency bands

step can cause problems because the selected values might not be well calibrated, even if they are biophysically plausible.

For example, all the selected numbers for the C parameters are proportions, and not the actual physical numbers of terminals that each neuron accepts. Further, the proportions themselves are approximations of the reality, and are expected to vary from subject to subject. Also, by using these numbers, we exclude the role of the distribution of terminals in somatic, proximal or distal areas, as well as important functional details of the effects of synaptic mechanisms, such as the shunting inhibition. On the contrary, these simplifications can be accepted as being consistent with the level of abstraction of the population modeling paradigm. Moreover, they provide a plausible relative picture of the sizes of the connections that should be considered in the modeling approaches of the basal ganglia.

Regarding the normal and parkinsonian firing rate activity of the model, there is no unique answer about what should be the target mean rates that should be captured. In the literature, many diverse reports about the levels of activation of the nuclei can be found, derived by a multitude of recording procedures in various species. That, together with the inevitable use of quantitative data from disparate sources for the parameters of the model, makes the effort to find a perfectly fitted and undisputable configuration unlikely. Therefore, we mostly think of the firing rate outputs of the populations as more qualitative rather than strict quantitative exhibitions of the simulated conditions.

Also, in the parkinsonian condition, the unified treatment of all the connections and all the receptor modules removed most of the many degrees of freedom that the model could possess if each connection was treated independently. Such an option, though, would lead in a huge number of possible cases and parametric configurations, and would obscure the core conclusions that can be drawn by the simulations.

Another simplification of the approach was the omission of the thalamus and other brain regions that interact with the basal ganglia, such as the pendunculopontine nucleus. An extension of the model that would include even more relevant structures and connections would be interesting, and we will consider it for future study.

We believe that all the conclusions drawn by the proposed model can provide valuable help for the identification of

the critical alterations of the physiology of the basal ganglia that lead to the parkinsonian condition. In addition, the understanding of the way that the DBS acts to ameliorate the symptoms may also be chased more effectively. According to Brown and Williams (2005), there are two possibilities to record LFPs from the basal ganglia, either through microelectrodes or directly from the DBS electrode. In the same review, it is stated that the basal ganglia's LFPs acquired by microelectrodes or bipolarly configured DBS macroelectrodes are focally generated, reflecting physiological activity of the same nature. Therefore, after the implantation of the stimulating DBS macroelectrode, LFP signals obtained by bipolar recordings can be compared to the model's output and give insights in a condition probably resembling the normal or drug-treated states.

Finally, the presented approach suggests that alternative therapeutic strategies for PD might be interesting to evaluate. For example, considering the notable success of the STN targeting DBS, inspired in essence by the classic direct–indirect pathway model, the proposed model seems to indicate another possible target; it points to a possibility toward the effectiveness of the DBS of the GPe, since this nucleus is also involved in the pathogenic oscillations dominating the basal ganglia, through the GPe–STN loop. The establishment of the reality of such a claim, though, may be pursued in parallel with targeted clinical and experimental studies about the mechanisms of DBS functioning, probably along with modeling studies of the basal ganglia and the DBS. Through such a clinical test, the model's validity could be also checked: If the DBS on the GPe turns out to an amelioration of the main kinetic symptoms, then this would be a first line of evidence in favor of the conclusions of the proposed model. Toward the trial clinical application of DBS on GPe, the development of DBS models that could work together with the proposed model might be very revealing, forming a very interesting perspective for future study.

Acknowledgements This study was supported by the Greek Secretariat of Research and Technology, under grant PENED 03ED512 (2006–2009), which is co-funded with 80% from the European Social Fund and by 20% from National funds. George L. Tsirogiannis has also been supported in part by the Bodossaki Foundation Graduate Scholarship (2004–2005).

References

Albin RL, Young AB, Penney JB (1989) The functional anatomy of basal ganglia disorders. Trends Neurosci 12: 366–375

Bamford NS, Robinson S, Palmiter RD, Joyce JA, Moore C, Meshul CK (2004) Dopamine modulates release from corticostriatal terminals. J Neurosci 24: 9541–9552

Barchas JD, Akil H, Elliott GR, Holman RB, Watson SJ (1978) Behavioral neurochemistry: neuroregulators and behavioral states. Science 200:964–973

Baufreton J, Zhu ZT, Garret M, Bioulac B, Johnson SW, Taupignon AI (2005) Dopamine receptors set the pattern of activity generated in subthalamic neurons. FASEB J 19: 1771–1777

Bauswein E, Fromm C, Preuss A (1989) Corticostriatal cells in comparison with pyramidal tract neurons: contrasting properties in the behaving monkey. Brain Res 493: 198–203

Beckstead RM, Wooten GF, Trugman JM (1988) Distribution of D1 and D2 dopamine receptors in the basal ganglia of the cat determined by quantitative autoradiography. J Comp Neurol 268: 131–145

Bedard C, Kroger H, Destexhe A (2006) Model of low-pass filtering of local field potentials in brain tissue. Phys Rev 73:051911

Benabid AL, Pollak P, Gervason C, Hoffmann D, Gao DM, Hommel M, Perret JE, de Rougemont J (1991) Long-term suppression of tremor by chronic stimulation of the ventral intermediate thalamic nucleus. Lancet 337: 403–406

Benazzouz A, Breit S, Koudsie A, Pollak P, Krack P, Benabid A-L (2002) Intraoperative microrecordings of the subthalamic nucleus in Parkinson's disease. Mov Disord 17: S145–S149

Bergman H, Deuschl G (2002) Pathophysiology of Parkinson's disease: from clinical neurology to basic neuroscience and back. Mov Disord 17: S28–S40

Bevan MD, Magill PJ, Terman D, Bolam JP, Wilson CJ (2002) Move to the rhythm: oscillations in the subthalamic nucleus–external globus pallidus network. Trends Neurosci 25: 525–531

Bolam JP, Hanley JJ, Booth PAC, Bevan MD (2000) Synaptic organization of the basal ganglia. J Anat 196: 527–542

Boraud T, Brown P, Goldberg JA, Graybiel AM, Magill PJ (2005) Oscillations in the basal ganglia: the good, the bad, and the unexpected. Basal Ganglia VIII: 3–24

Brown P (2003) Oscillatory nature of human basal ganglia activity: relationship to the pathophysiology of Parkinson's disease. Mov Disord 18: 357–363

Brown P, Williams D (2005) Basal ganglia local field potential activity: character and functional significance in the human. Clin Neurophysiol 116: 2510–2519

Brown P, Kupsch A, Magill PJ, Sharott A, Harnack D, Meissner W (2002) Oscillatory local field potentials recorded from the subthalamic nucleus of the alert rat. Exp Neurol 177: 581–585

Bullock TH (1997) Signals and signs in the nervous system: the dynamic anatomy of electrical activity is probably information-rich. Proc Natl Acad Sci USA 94: 1–6

Calabresi P, Centonze D, Bernardi G (2000) Electrophysiology of dopamine in normal and denervated striatal neurons. Trends Neurosci 23: 57–63

Carpenter MB, Carleton SC, Keller JT, Conte P (1981) Connections of the subthalamic nucleus in the monkey. Brain Res 224: 1–29

Cepeda C, Andre VM, Yamazaki I, Wu N, Kleiman-Weiner M, Levine MS (2008) Differential electrophysiological properties of dopamine D1 and D2 receptor-containing striatal medium-sized spiny neurons. Eur J Neurosci 27: 671–682

Charara A, Sidibe M, Smith Y (2003) Basal ganglia circuitry and synaptic connectivity. In: Tarsy D, Vitek JL, Lozano AM (eds) Contemporary clinical neurology: surgical treatment of Parkinson's disease and other movement disorders. Humana Press, pp 19–39

Chen CC, Pogosyan A, Zrinzo LU, Tisch S, Limousin P, Ashkan K, Yousry T, Hariz MI, Brown P (2006) Intra-operative recordings of local field potentials can help localize the subthalamic nucleus in Parkinson's disease surgery. Exp Neurol 198: 214–221

Choe Y, Miikkulainen R (2003) The role of postsynaptic potential decay rate in neural synchrony. Neurocomputing 52–54: 707–712

Cooper AJ, Stanford IM (2000) Electrophysiological and morphological characteristics of three subtypes of rat globus pallidus neurone in vitro. J Physiol 527: 291–304

Cooper AJ, Stanford IM (2001) Dopamine D2 receptor mediated presynaptic inhibition of striatopallidal GABAA IPSCs in vitro. Neuropharmacology 41: 62–71

Cosandier-Rimele D, Badier JM, Chauvel P, Wendling F (2007) A physiologically plausible spatio-temporal model for EEG signals recorded with intracerebral electrodes in human partial epilepsy. IEEE Trans Biomed Eng 54: 380–388

Czubayko U, Plenz D (2002) Fast synaptic transmission between striatal spiny projection neurons. Proc Natl Acad Sci 99: 15764–15769

Dostrovsky J, Bergman H (2004) Oscillatory activity in the basal ganglia—relationship to normal physiology and pathophysiology. Brain 127: 721–722

Elson RC, Selverston AI, Abarbanel HDI, Rabinovich MI (2002) Inhibitory synchronization of bursting in biological neurons: dependence on synaptic time constant. J Neurophysiol 88: 1166–1176

Falls WM, Park MR, Kitai ST (1983) An intracellular HRP study of the rat globus pallidus. II. Fine structural characteristics and synaptic connections of medially located large GP neurons. J Comp Neurol 221: 229–245

Floran B, Floran L, Erlij D, Aceves J (2004) Dopamine D4 receptors inhibit depolarization-induced [3H]GABA release in the rat subthalamic nucleus. Eur J Pharmacol 498: 97–102

Freeman WJ (1978) Models of the dynamics of neural populations. Electroencephalogr Clin Neurophysiol 34: 9–18

Freeman WJ (2000) Characteristics of the synchronization of brain activity imposed by finite conduction velocities of axons. Int J Bifurc Chaos 10: 2307–2322

Gerstner W, Kistler W (2002) Spiking neuron models: an introduction. Cambridge University Press, New York

Gillies A, Willshaw D (2004) Models of the subthalamic nucleus. The importance of intranuclear connectivity. Med Eng Phys 26: 723–732

Gopalsamy K, Leung I (1996) Delay induced periodicity in a neural netlet of excitation and inhibition. Physica D 89: 395–426

Gotz T, Kraushaar U, Geiger J, Lubke J, Berger T, Jonas P (1997) Functional properties of AMPA and NMDA receptors expressed in identified types of basal ganglia neurons. J Neurosci 17: 204–215

Gurney K, Prescott TJ, Redgrave P (2001) A computational model of action selection in the basal ganglia. I. A new functional anatomy. Biol Cybern 84:401–410

Haber SN (2008) Functional anatomy and physiology of the basal ganglia: non-motor functions. In: Tarsy D, Vitek JL, Starr PA, Okun MS (eds) Deep brain stimulation in neurological and psychiatric disorders. Humana Press, pp 33–62

Hamani C, Saint-Cyr JA, Fraser J, Kaplitt M, Lozano AM (2004) The subthalamic nucleus in the context of movement disorders. Brain 127: 4–20

Hammond C, Bergman H, Brown P (2007) Pathological synchronization in Parkinson's disease: networks, models and treatments. Trends Neurosci 30: 357–364

Humphries MD, Stewart RD, Gurney KN (2006) A physiologically plausible model of action selection and oscillatory activity in the basal ganglia. J Neurosci 26: 12921–12942

Jansen BH, Rit VG (1995) Electroencephalogram and visual evoked potential generation in a mathematical model of coupled cortical columns. Biol Cybern 73: 357–366

Jansen BH, Zouridakis G, Brandt ME (1993) A neurophysiologically-based mathematical model of flash visual evoked potentials. Biol Cybern 68: 275–283

Johnson PI, Napier TC (1997) GABA-and glutamate-evoked responses in the rat ventral pallidum are modulated by dopamine. Eur J Neurosci 9: 1397–1406

Johnston D, Wu SM (1995) Foundations of cellular neurophysiology. MIT Press, Cambridge

Kincaid AE, Zheng T, Wilson CJ (1998) Connectivity and convergence of single corticostriatal axons. J Neurosci 18: 4722–4731

Kita H, Kitai ST (1991) Intracellular study of rat globus pallidus neurons: membrane properties and responses to neostriatal, subthalamic and nigral stimulation. Brain Res 564: 296–305

Kita H, Kita T, Kitai ST (1985) Active membrane properties of rat neostriatal neurons in an in vitro slice preparation. Exp Brain Res 60: 54–62

Kreiss DS, Mastropietro CW, Rawji SS, Walters JR (1997) The response of subthalamic nucleus neurons to dopamine receptor stimulation in a rodent model of Parkinson's disease. J Neurosci 17: 6807–6819

Kuhn AA, Kupsch A, Schneider GH, Brown P (2006) Reduction in subthalamic 8–35 Hz oscillatory activity correlates with clinical improvement in Parkinson's disease. Eur J Neurosci 23:1956–1960

Kuhn AA, Kempf F, Brucke C, Gaynor Doyle L, Martinez-Torres I, Pogosyan A, Trottenberg T, Kupsch A, Schneider GH, Hariz MI et al (2008) High-frequency stimulation of the subthalamic nucleus suppresses oscillatory β activity in patients with Parkinson's disease in parallel with improvement in motor performance. J Neurosci 28: 6165–6173

Lange KW, Kornhuber J, Riederer P (1997) Dopamine/glutamate interactions in Parkinson's disease. Neurosci Biobehav Rev 21:393–400

Limousin P, Pollak P, Benazzouz A, Hoffmann D, Le Bas JF, Broussolle E, Perret JE, Benabid AL (1995) Effect of parkinsonian signs and symptoms of bilateral subthalamic nucleus stimulation. Lancet 345: 91–95

Liu X (2003) What can be learned from recording local field potentials from the brain via implanted electrodes used to treat patients with movement disorders. Curr Med Lit 19: 1–6

Logothetis NK, Kayser C, Oeltermann A (2007) In vivo measurement of cortical impedance spectrum in monkeys: implications for signal propagation. Neuron 55: 809–823

Lopes da Silva FH, Hoeks A, Smits H, Zetterberg LH (1974) Model of brain rhythmic activity. Biol Cybern 15: 27–37

Lopes da Silva FH, van Rotterdam A, Barts P, van Heusden E, Burr W (1976) Models of neuronal populations: the basic mechanisms of rhythmicity. Prog Brain Res 45: 281–308

Mallet N, Pogosyan A, Sharott A, Csicsvari J, Bolam JP, Brown P, Magill PJ (2008) Disrupted dopamine transmission and the emergence of exaggerated beta oscillations in subthalamic nucleus and cerebral cortex. J Neurosci 28:4795

Missale C, Nash SR, Robinson SW, Jaber M, Caron MG (1998) Dopamine receptors: from structure to function. Physiol Rev 78: 189–225

Nakanishi H, Kita H, Kitai ST (1987) Electrical membrane properties of rat subthalamic neurons in an in vitro slice preparation. Brain Res 437: 35–44

Nakanishi H, Kita H, Kitai ST (1990) Intracellular study of rat entopeduncular nucleus neurons in an in vitro slice preparation: electrical membrane properties. Brain Res 527: 81–88

Nambu A (2005) A new approach to understand the pathophysiology of Parkinson's disease. J Neurol 252(Suppl 4): IV/1–IV/4

Nambu A, Llinas R (1994) Electrophysiology of globus pallidus neurons in vitro. J Neurophysiol 72: 1127–1139

Nambu A, Tokuno H, Takada M (2002) Functional significance of the cortico-subthalamo-pallidal 'hyperdirect' pathway. Neurosci Res 43: 111–117

Nunez PL, Srinivasan R (2006) Electric fields of the brain: the neurophysics of EEG. Oxford University Press, Oxford

Orieux G, Francois C, Feger J, Yelnik J, Vila M, Ruberg M, Agid Y, Hirsch EC (2000) Metabolic activity of excitatory parafascicular and pedunculopontine inputs to the subthalamic nucleus in a rat model of Parkinson's disease. Neuroscience 97: 79–88

Parent A (1986) Comparative neurobiology of the basal ganglia. Wiley, New York

Parent A, Hazrati LN (1995) Functional anatomy of the basal ganglia. I. The corticobasal gangliathalamocortical loop. Brain Res Rev 20:91127

Penney JB, Young AB (1983) Speculations on the functional anatomy of basal ganglia disorders. Annu Rev Neurosci 6: 73–94

Pollack AE (2001) Anatomy, physiology, and pharmacology of the basal ganglia. Neurol Clin 19: 523–534

Priori A, Egidi M, Pesenti A, Rohr M, Rampini P, Locatelli M, Tamma P, Caputo E, Chiesa V, Barbieri S (2003) Do intraoperative microrecordings improve subthalamic nucleus targeting in stereotactic neurosurgery for Parkinson's disease?J Neurosurg Sci 47: 56–60

Priori A, Foffani G, Pesenti A, Tamma F, Bianchi AM, Pellegrini M, Locatelli M, Moxon KA, Villani RM (2004) Rhythm-specific pharmacological modulation of subthalamic activity in Parkinson's disease. Exp Neurol 189: 369–379

Ravenscroft P, Brotchie J (2000) NMDA receptors in the basal ganglia. J Anat 196: 577–585

Rinzel J, Terman D, Wang XJ, Ermentrout B (1998) Propagating activity patterns in large-scale inhibitory neuronal networks. Science 279: 1351–1355

Sato F, Parent M, Levesque M, Parent A (2000) Axonal branching pattern of neurons of the subthalamic nucleus in primates. J Comp Neurol 424: 142–152

Seamans J, Durstewitz D (2008) Dopamine modulation. Scholarpedia 3:2711

Sharott A, Magill PJ, Harnack D, Kupsch A, Meissner W, Brown P (2005) Dopamine depletion increases the power and coherence of beta-oscillations in the cerebral cortex and subthalamic nucleus of the awake rat. Eur J Neurosci 21: 1413–1422

Shen KZ, Johnson SW (2000) Presynaptic dopamine D2 and muscarine M3 receptors inhibit excitatory and inhibitory transmission to rat subthalamic neurones in vitro. J Physiol 525: 331–341

Shen KZ, Johnson SW (2006) Subthalamic stimulation evokes complex EPSCs in the rat substantia nigra pars reticulata in vitro. J Physiol 573: 697–709

Shen KZ, Zhu ZT, Munhall A, Johnson SW (2003) Dopamine receptor supersensitivity in rat subthalamus after 6-hydroxydopamine lesions. Eur J Neurosci 18: 2967–2974

Shink E, Smith Y (1995) Differential synaptic innervation of neurons in the internal and external segments of the globus pallidus by the GABA-and glutamate-containing terminals in the squirrel monkey. J Comp Neurol 358: 119–141

Smith Y, Kieval JZ (2000) Anatomy of the dopamine system in the basal ganglia. Trends Neurosci 23:28–33

Smith Y, Wichmann T (2008) Functional anatomy and physiology of the basal ganglia: motor functions. In: Tarsy D, Vitek JL, Starr PA, Okun MS (eds) Deep brain stimulation in neurological and psychiatric disorders. Humana Press, pp 1–32

Smith Y, Bevan MD, Shink E, Bolam JP (1998) Microcircuitry of the direct and indirect pathways of the basal ganglia. Neuroscience 86:353–387

Terman D, Rubin JE, Yew AC, Wilson CJ (2002) Activity patterns in a model for the subthalamopallidal network of the basal ganglia. J Neurosci 22:2963–2976

Trottenberg T, Kupsch A, Schneider GH, Brown P, Kuhn AA (2007) Frequency-dependent distribution of local field potential activity within the subthalamic nucleus in Parkinson's disease. Exp Neurol 205:287–291

Utter AA, Basso MA (2008) The basal ganglia: an overview of circuits and function. Neurosci Biobehav Rev 32:333–342

Van Albada SJ, Robinson PA (2009) Mean-field modeling of the basal ganglia-thalamocortical system. I Firing rates in healthy and parkinsonian states. J Theor Biol 257:642–663

Van Rotterdam A, Lopes da Silva FH, Van den Ende J, Viergever MA, Hermans AJ (1982) A model of the spatial-temporal characteristics of the alpha rhythm. Bull Math Biol 44:283–305

Vibert JF, Parkdaman K, Azmy N (1994) Interneural delay modification synchronizes biologically plausible neural networks. Neural Netw 7:589–607

Vibert JF, Alvarez F, Pham J (1998) Effects of transmission delays and noise in recurrent excitatory neural networks. Biosystems 48:255–262

Walters JR, Hu D, Itoga CA, Parr-Brownlie LC, Bergstrom DA (2006) Phase relationship support a role for coordinated activity in the indirect pathway in organizing slow oscillations in basal ganglia output after loss of dopamine. Neuroscience 144:762–776

Weinberger M, Mahant N, Hutchison WD, Lozano AM, Moro E, Hodaie M, Lang AE, Dostrovsky JO (2006) Beta oscillatory activity in the subthalamic nucleus and its relation to dopaminergic response in Parkinson's disease. J Neurophysiol 96: 3248–3256

Wendling F, Bellanger JJ, Bartolomei F, Chauvel P (2000) Relevance of nonlinear lumped-parameter models in the analysis of depth-EEG epileptic signals. Biol Cybern 83: 367–378

Wendling F, Bartolomei F, Bellanger JJ, Chauvel P (2002) Epileptic fast activity can be explained by a model of impaired GABAergic dendritic inhibition. Eur J Neurosci 15: 1499–1508

West AR, Grace AA (2002) Opposite influences of endogenous dopamine D1 and D2 receptor activation on activity states and electrophysiological properties of striatal neurons: studies combining in vivo intracellular recordings and reverse microdialysis. J Neurosci 22:294

Wichmann T, DeLong MR (2006) Basal ganglia discharge abnormalities in Parkinson's disease. J Neural Transm [Suppl] 70: 21–25

Wingeier B, Tcheng T, Koop MM, Hill BC, Heit G, Bronte-Stewart HM (2006) Intra-operative STN DBS attenuates the prominent beta rhythm in the STN in Parkinson's disease. Exp Neurol 197: 244–251

Yasumoto S, Tanaka E, Hattori G, Maeda H, Higashi H (2002) Direct and indirect actions of dopamine on the membrane potential in medium spiny neurons of the mouse neostriatum. J Neurophysiol 87: 1234–1243